Deep-Sea Research I 75 (2013) 157–174

Contents lists available at SciVerse ScienceDirect

Deep-Sea Research I

journal homepage: www.elsevier.com/locate/dsri

Morphosedimentary and hydrographic features of the northern Argentine margin: The interplay between erosive, depositional and gravitational processes and its conceptual implications

Benedict Preu [a,*], F. Javier Hernández-Molina [b], Roberto Violante [c], Alberto R. Piola [d,e], C. Marcelo Paterlini [f], Tilmann Schwenk [a], Ines Voigt [a], Sebastian Krastel [g,1], Volkhard Spiess [a]

[a] MARUM – Center for Marine Environmental Sciences and Faculty of Geosciences, University of Bremen, Germany
[b] Facultad de Ciencias de Mar, Universidad de Vigo, Vigo, Spain
[c] Sección Geología Marina, Servicio de Hidrografia Naval (SHN), Buenos Aires, Argentina
[d] Sección Dinámica Oceánica, Servicio de Hidrografia Naval (SHN), Buenos Aires, Argentina
[e] Universidad de Buenos Aires, and Instituto Franco-Argentino sobre Estudios de Clima y sus Impactos, CONICET, Buenos Aires, Argentina
[f] Sección Geofísica Marina, Servicio de Hidrografia Naval (SHN), Buenos Aires, Argentina
[g] GEOMAR/Helmholtz Centre for Ocean Research Kiel, Kiel, Germany

ARTICLE INFO

Article history:
Received 9 July 2012
Received in revised form
14 December 2012
Accepted 23 December 2012
Available online 16 January 2013

Keywords:
Contourite drift
Contourite terraces
Water mass interfaces
Erosive surface
Brazil–Malvinas Confluence

ABSTRACT

Bottom currents and their margin-shaping character became a central aspect in the research field of sediment dynamics and paleoceanography during the last decades due to their potential to form large contourite depositional systems (CDS), consisting of both erosive and depositional features.

A major CDS at the northern Argentine continental margin was studied off the Rio de la Plata River by means of seismo- and hydro-acoustic methods including conventional and high-resolution seismic, parametric echosounder and single and swath bathymetry. Additionally, hydrographic data were considered allowing jointly interpretation of morphosedimentary features and the oceanographic framework, which is dominated by the presence of the dynamic and highly variable Brazil–Malvinas Confluence.

We focus on three regional contouritic terraces identified on the slope in the vicinity of the Mar del Plata Canyon. The shallowest one, the La Plata Terrace (~500 m), is located at the Brazil Current/Antarctic Intermediate Water interface characterized by its deep and distinct thermocline. In ~1200 m water depth the Ewing Terrace correlates with the Antarctic Intermediate Water/Upper Circumpolar Deep Water interface. At the foot of the slope in ~3500 m the Necochea Terrace marks the transition between Lower Circumpolar Deep Water and Antarctic Bottom Water during glacial times.

Based on these correlations, a comprehensive conceptual model is proposed, in which the onset and evolution of contourite terraces is controlled by short- and long-term variations of water mass interfaces. We suggest that the terrace genesis is strongly connected to the turbulent current pattern typical for water mass interfaces. Furthermore, the erosive processes necessary for terrace formation are probably enhanced due to internal waves, which are generated along strong density gradients typical for water mass interfaces. The terraces widen through time due to locally focused, partly helical currents along the steep landward slopes and more tabular conditions seaward along the terrace surface.

Considering this scheme of contourite terrace development, lateral variations of the morphosedimentary features off northern Argentina can be used to derive the evolution of the Brazil–Malvinas Confluence on geological time scales. We propose that the Brazil–Malvinas Confluence in modern times is located close to its southernmost position in the Quaternary, while its center was shifted northward during cold periods.

* Corresponding author. Tel.: +49 421 218 65376, fax: +49 421 218 65399.
E-mail addresses: bpreu@uni-bremen.de (B. Preu), fjhernan@uvigo.es (F.J. Hernández-Molina), violante@hidro.gov.ar (R. Violante), apiola@hidro.gov.ar (A.R. Piola), mpaterlini@hidro.gov.ar (C.M. Paterlini), tschwenk@uni-bremen.de (T. Schwenk), ivoigt@uni-bremen.de (I. Voigt), skrastel@ifm-geomar.de (S. Krastel), vspiess@uni-bremen.de (V. Spiess).
[1] Now at Department of Geosciences, University of Kiel, Germany.

0967-0637/$ - see front matter © 2013 Elsevier Ltd. All rights reserved.
http://dx.doi.org/10.1016/j.dsr.2012.12.013

1. Introduction

Bottom currents represent a major force shaping ocean margins (e.g. Heezen, 1959; Heezen and Hollister, 1964; Stow et al., 2009) through along-slope oceanographic processes, which are capable of eroding, transporting, and depositing sediments at the seafloor (Rebesco and Camerlenghi, 2008). Depending on the bottom relief, local and regional hydrodynamic features (cores, branches, vortices, helical flows, etc.) might develop, which dominate sedimentary processes (Hernández-Molina et al., 2008a). A sufficiently strong bottom current acting over an extended time period will profoundly affect the seabed, ranging from winnowing of fine-grained sediments to large-scale erosion and deposition (e.g., Heezen, 1959; Heezen and Hollister, 1964; Stow and Lovell, 1979; Viana and Faugères, 1998; Duarte and Viana, 2007; Rebesco and Camerlenghi, 2008; Stow et al., 2009).

The term 'contourite' is now generally accepted for those sediments deposited or substantially reworked by bottom currents (Stow et al., 2002; Rebesco, 2005; Rebesco and Camerlenghi, 2008; Faugères and Mulder, 2011). Major accumulations of contourite deposits are referred to as drifts or contourite drifts, for which several classifications have been proposed based mainly on their morphological, sedimentological and internal architecture (e.g.,: McCave and Tucholke, 1986; Faugères et al., 1993, 1999; Stow et al., 2002; Rebesco, 2005; Rebesco and Camerlenghi, 2008; Faugères and Mulder, 2011).

Where currents are strong enough, a variety of erosive features can develop. Extensive erosion or non-deposition leads to the development of widespread hiatuses in the depositional record. Although erosive features are not as well studied as contourite drifts, several types have been investigated to date (e.g., Nelson et al., 1993, 1999; Stow and Mayall, 2000; Hernández-Molina et al., 2003, 2008a, 2009; Stow et al., 2008, 2009; García et al., 2009). The most common are represented by erosive surfaces associated with contourite terraces. An association of various drifts and related erosive features is commonly termed a Contourite Depositional System (CDS), by analogy with, and of equal importance as, Turbidite Depositional Systems (e.g., Hernández-Molina et al., 2003, 2008a).

A huge CDS extends along the Argentine margin characterized by particularly well developed depositional and erosive features (Hernández-Molina et al., 2009). In regional studies, contourite features were so far mainly identified in the southernmost sector of the margin (Hernández-Molina et al., 2009, 2010; Lastras et al., 2011; Gruetzner et al., 2012). However, recently Violante et al. (2010), Bozzano et al. (2011), Krastel et al. (2011) and Preu et al. (2012) have also reported large contourite features along the northern Argentine margin.

The main objective of this work is to identify and discuss morphosedimentary features along the northern Argentine margin (Fig. 1) with special emphasis on contourite terraces, which are present in different depths along the slope. A regional correlation with hydrographic features is presented and a new conceptual model for the onset and evolution of contourite terraces is discussed.

2. Regional setting

2.1. Physiography

The Argentine continental margin (Fig. 1) includes three major physiographic domains: the shelf, the slope and the rise. All three margin segments, which were investigated in several regional studies (e.g., Ewing and Lonardi, 1971; Lonardi and Ewing, 1971; Parker et al., 1996, 1997; Hernández-Molina et al., 2009) include morphological features, which are relevant indicators for the interaction between ocean dynamics, tectonic processes, sea level

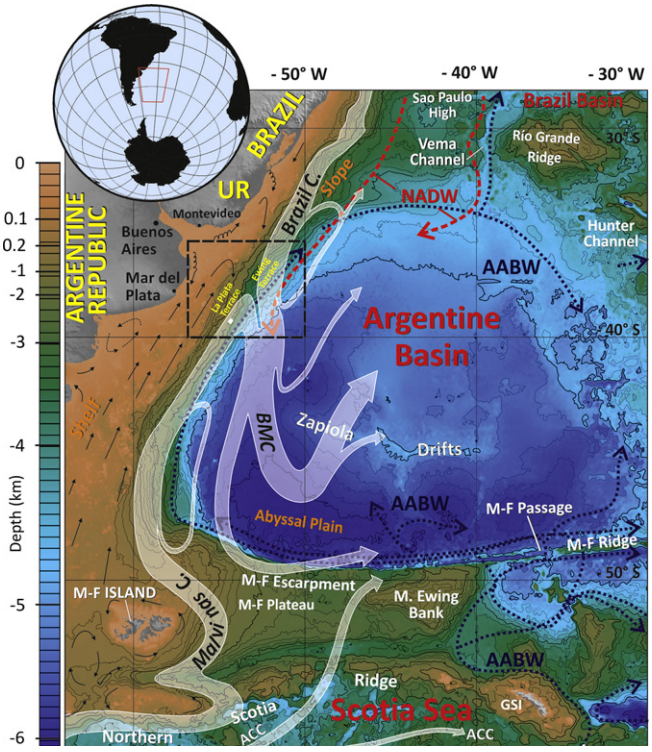

Fig. 1. Regional map of the NE Argentine continental margin, including its general ocean circulation pattern; AABW—Antarctic Bottom Water; ACC—Antarctic Circumpolar Current; BMC—Brazil–Malvinas Confluence; M-F—Malvinas–Falkland; NADW—North Atlantic Deep Water; GSI: South Georgia; black dashed box marks the study area.

fluctuations and partly gravitational processes (e.g., Urien and Ewing, 1974; Violante and Parker, 2004; Hernández-Molina et al., 2009, 2010; Henkel et al., 2011; Krastel et al., 2011).

The shelf varies in its width from north to south (Ewing and Lonardi, 1971; Parker et al., 1996, 1997). The narrowest part of the shelf in the study area is located near Mar del Plata and further south where the shelf is ~180 km wide (Fig. 1). South of this area the continental shelf width exceeds 200 km. The eastern boundary of the shelf is close to a straight line, which runs in SSW direction along the 130/150 m isobaths in the study area.

The slope strikes in a NE-SW direction in the study area. In this part of the margin the slope extends over ~180 km in width with a mean slope angle of 2–5°. Located off the Rio de la Plata (Fig. 1), two major terraces result in a step-like slope morphology by the La Plata Terrace (Urien and Ewing, 1974) and the Ewing Terrace (Hernández-Molina et al., 2009). The latter encompasses significant sediment accumulations (Violante et al., 2010).

2.2. Oceanographic context

Interaction of highly active oceanographic processes with the seafloor is a ubiquitous characteristic of the Argentine margin, which is one of the most dynamic regions of the world ocean (e.g., Chelton et al., 1990). This margin encompasses the Brazil–Malvinas Confluence (BMC, Fig. 1), as well as the encounter and interaction of northward flowing Antarctic water masses (Antarctic Intermediate Water [AAIW], Upper Circumpolar Deep Water [UCDW], Lower Circumpolar Deep Water [LCDW] and Antarctic Deep Water [AABW]), with the southward flowing Brazil Current (BC), which contains fractions of Tropical Water and South Atlantic Central Water (SACW), re-circulated AAIW and North Atlantic Deep Water (NADW, Saunders and King, 1995; Georgi, 1981; Piola and Matano, 2001; Carter and Cortese, 2009) at different depths.

The surface circulation along the Argentine margin results from interaction of the northward flowing Malvinas Current with the southward flowing Brazil Current, which form the BMC near 38°S (Fig. 1). South of the BMC the intermediate and deep circulation is conditioned by the northward flow of AAIW, UCDW and LCDW (Reid et al., 1977; Arhan et al., 2002, 2003). North of the confluence, the NADW flows southward along the margin. The interfaces between these water masses are characterized by relatively large vertical density gradients. At basin scale these interfaces tend to deepen northward (Reid et al., 1977), and are vertically displaced by eddies (Piola and Matano, 2001; Arhan et al., 2002, 2003).

The abyssal circulation is dominated by the AABW (Fig. 1), which is partially trapped in the Argentine basin. This trapping generates a large, regionally up to 2000 m thick cyclonic gyre, whose influence is apparent at depths greater than 3500 to 4000 m (Piola and Matano, 2001; Arhan et al., 2002, 2003; Hernández-Molina et al., 2008b; Carter and Cortese, 2009). These circulation patterns may play a significant role in controlling sedimentary processes across the entire ocean basin (Le Pichon et al., 1971; Klaus and Ledbetter, 1988; Reid, 1989), and particularly on the Argentine margin (Flood and Shor, 1988; Arhan et al., 2002, 2003; Hernández-Molina et al., 2009).

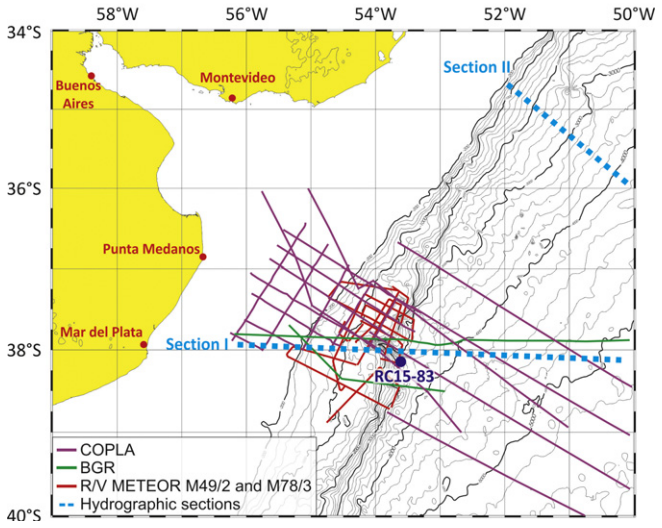

Fig. 2. Map of study area showing the position of the seismic surveys (COPLA, BGR, R/V Meteor) and the water column data including hydrographic sections (Fig. 6) and turbidity measurements (RC15-83, Fig. 10).

2.3. Geological context

The northern part of the Argentine margin belongs to the passive volcanic rifted continental margin of South America ranging from southern Brazil to northern Patagonia. The tectonic characteristics of the region are conditioned by deep structures related to the geodynamic evolution prior to the continental fragmentation, as well as by sea-floor spreading, magmatic activity and thermal flux (Ramos, 1999). The margin has been subdivided into four tectonic segments separated each other by transfer fracture zones (Hinz et al., 1999; Franke et al., 2007). The study area comprises the northern part of Segment III and the southern part of Segment IV, which are separated by the Salado Transfer Zone (STZ, Supplement 1).

Post-Cretaceous sedimentary sequences display six major units separated by conspicuous seismic horizons. Sequences between reflectors indicate the different stages of evolution (Ewing and Lonardi, 1971; Urien and Zambrano, 1996; Hinz et al.,1999; Parker et al., 2008; Violante et al., 2010; Preu et al., 2012): (1) a first stage (Early Cenozoic) characterized by a high vertical accretion of the slope; (2) a second stage (Eocene-Mid Miocene), when the passive margin definitively developed, Antarctic water-masses began to actively influence the region, and prograding–retrograding sedimentary sequences played a significant role in shaping and enlarging the slope with high turbiditic dynamic and formation of submarine canyons; (3) the third stage (Mid-Late Miocene) comprises the time-span when progradation dominated, major regional tectonic, stratigraphic and paleoceanographic changes took place and ocean and sediment dynamics gave rise to contouritic sedimentation with the formation of the Ewing Terrace; (4) finally, the fourth stage (Late Pliocene—Quaternary) represents the definitive morphosedimentary evolution of the slope towards its present characteristics, with intense contouritic and turbiditic activity and the final excavation of the Mar del Plata Submarine Canyon.

3. Methods

3.1. Seismic and hydro-acoustic data sets

Multiple seismo- and hydroacoustic data sets covering a wide range of frequencies were used in order to analyze small scale variations in morphology and seismo-acoustic facies of the shallow subseafloor and to investigate possible links to the recent oceanographic regime. Conventional and high-resolution multichannel seismic (MCS) profiles, single- and multibeam lines and parametric echosounder data were analyzed and jointly interpreted (Fig. 2).

The conventional MCS (10–50 Hz) data were provided by the *Comisión Nacional del Límite Exterior de la Plataforma Continental* (COPLA, Argentina). Partly, the data were acquired and processed by the *Bundesanstalt für Geowissenschaften und Rohstoffe* (BGR) to study the volcanic activity along the Argentine margin during the continental breakup (Hinz et al., 1999; Franke et al., 2007). The shooting interval during all BGR cruises (Fig. 2) was 50 m and data were recorded using a 6000 m long streamer system, sampled at a rate of 2 ms. The data were reprocessed on behalf of COPLA by CGG/VERITAS. These data were used in the background to identify potential structural control on margin physiography and consequently on morphosedimentary features.

High-resolution MCS (100–500 Hz) profiles were recorded during R/V Meteor Cruises M49/2 (2001) and M78/3 (2009). During the first cruise data were acquired using the multichannel seismic system of the University of Bremen encompassing a 600 m analog streamer with 96 channels. The sampling frequency was set to 4 kHz (Spieß et al., 2002). In 2009 data were recorded with the GEOMAR multichannel seismic system using a 200 m-long digital streamer consisting of 128 channels. Sample frequency during that cruise was constantly 8 kHz (Krastel and Wefer, 2011). Both data sets were processed with the software package 'VISTA Seismic Processing 2D/3D' (GEDCO) following standard seismic procedures including bandpass filtering, common midpoint (CMP) sorting and binning, CMP stacking, residual static correction and post-stack time migration. CMP bin size varies among profiles between 5 and 10 m depending on data quality and coverage. Based on these data large scale erosive and depositional features were identified and mapped within the study area.

Single beam echosounder data were collected by Argentine authorities on behalf of COPLA during multiple cruises with R/V Puerto Deseado during the last decade (not shown in Fig. 2). This data set was analyzed in conjunction with a dense multibeam echosounder data set confined to the Mar del Plata Canyon, recorded during R/V Meteor Cruise M78/3, in order to determine large and small-scale morphological features. Additionally,

parametric sediment echosounder data (PARASOUND P70 with a lower parametric frequency of 4 kHz) acquired along the multibeam tracks were used for detailed morphological and seismo-acoustic analysis of the uppermost tens of meters (Krastel and Wefer, 2011).

To discuss the origin, evolution and lateral extent of the morphosedimentary features, acoustic data sets were jointly interpreted using the software package 'The Kingdom Software' (SMT) and the software 'GeoMapApp' created at the Lamont-Doherty Earth Observatory (Ryan et al., 2009).

Identification of erosive and depositional features related to CDSs and the related nomenclature are based on previous comprehensive and reviewing studies carried out by Faugères et al. (1999) and Rebesco (2005). Both publications were recently summarized and discussed by Rebesco and Camerlenghi (2008).

3.2. Hydrographic data sets

The detailed distribution of water masses down the northern portion of the Argentine margin is depicted by two full-depth, high-resolution cross-sections of potential temperature (θ), salinity (S), dissolved oxygen (O_2) and neutral density (γ^n) (location indicated in Fig. 2). Section 1 was collected close to 38°S in 1984 as part of the Marathon Expedition (Camp et al., 1985) and Section 2, gathered further north during the SAVE-5 Expedition (Anonymous, 1992), runs southeastwards down the slope intersecting the 2000 m isobath near 35°S (Fig. 2). Note that the cross-slope resolution of Section 1 is about 30 km, while that of Section 2 east of the 200 m isobath is quite lower and irregular. Both sections were used to identify lateral changes in circulation based on distinct variations in water mass distributions over the study area.

As pointed out above, the abyssal Argentine Basin is subject to the influence of the circulation of AABW; however, as bottom depth decreases across the continental margin, various water masses interact with the seafloor. To understand the role of the circulation and water mass structure on the sediment redistribution over the slope it is necessary to determine where each water mass interacts with the bottom across and along the slope. For this purpose we analyzed the distribution of near-bottom (within 150 m) water mass properties based on all data available (World Ocean Database, 2009) in the Argentine Basin. The choice of the deepest 150 m slab arises from the need to determine the water mass in contact with the bottom and the need to have enough observations to depict their horizontal extent along the slope. We adopted water mass property criteria as shown in Table 1.

To allow detailed analysis of the interplay between the oceanography and the morphosedimentary features, the hydrographic sections and seismic lines were combined into single profiles. These seismic/hydrographic intersections were calculated using the program 'Ocean Data View 4.0' (Schlitzer, 2011).

Table 1
Selected criteria used to determine the ranges of the water masses interacting with the ocean bottom on the western margin of the Argentine Basin. θ: potential temperature (°C), S: salinity, O_2: dissolved oxygen (ml/l), γ^n: neutral density (kg/m^3).

Water mass	Criteria	
SACW	$\theta > 8$	$S > 34.8$
AAIW	$33.90 < S < 34.25$	
AAIW (recirc.)	$O_2 < 5.6$ ml/l	
UCDW	$27.75 < \gamma^n < 27.90$	$O_2 < 4.5$ ml/l
NADW	$27.90 < \gamma^n < 28.10$	$S > 34.8$
LCDW	$28.06 < \gamma^n < 28.20$	$S < 34.8$
AABW	$\theta < 0$ °C	

Additionally, sea surface temperature (SST) measurements were used for this study derived from published high-resolution satellite climatology (Casey and Cornillon, 1999). Based on these data, SST gradients were calculated and averaged to southern hemisphere summer (October–March) and winter (April–September) to visualize the seasonal variability of the BMC.

4. Results

4.1. Physiography of the study area

In the study area the continental slope varies in width between 160 and 200 km. It clearly narrows north of the Mar del Plata Submarine Canyon (Fig. 3), which separates the southern from the northern part of the study area. The continental slope can be subdivided into upper, middle and lower slope, which include several major terraces (Fig. 3): the La Plata Terrace (T1, 500–600 m), the Ewing Terrace (T2, 1200–1500 m) and the Necochea Terrace (T4, ~3500 m). Although another terrace (T3, 2500 m) has been described and regionally characterized by Hernández-Molina et al. (2011), this terrace will not be considered in this study due to its small-scale appearance in the study area.

The region where the lower slope merges with the continental rise is sometimes hard to identify due to a constant concave shape of the continental slope; however, the transition is located close to ~3500 m water depth, where slope angles reach ~0.6°. The continental rise covers an extensive area with an overall width of more than 200 km.

Three major submarine canyons are located in the study area (Fig. 3): The most prominent is the Mar del Plata Submarine Canyon, which originates at ~1000 m water depth cutting into the middle slope and reaches toward the foot of the lower slope (Krastel et al., 2011). The head of the Mar del Plata Canyon is located in the middle slope, mid-way between the La Plata and the Ewing Terrace (Fig. 3). The canyon has a length of ~130 km and is almost 18 km wide in the center of the Ewing Terrace.

North of the Mar del Plata Canyon a smaller structure, called Querandi Submarine Canyon, is incised into the Ewing Terrace and the lower slope. A much smaller canyon structure originates from the lower slope south of the Mar del Plata Canyon, called Punta Mogotes Submarine Canyon (Fig. 3).

4.2. Morphosedimentary features

4.2.1. Erosive features

Sedimentary features in the study area encompass erosive surfaces, channels and minor slope-parallel incisions located at the lower slope. Overall these features are very pronounced in the northern and southern part of the study area (Figs. 3 and 4).

4.2.1.1. Erosive surfaces. Two major large-scale erosional surfaces were imaged in the northern and southern part of the study area, one represented by the upper slope landward of the La Plata Terrace and the other one located along the middle slope located seaward of the La Plata Terrace (Figs. 3, 4a and b, 5a and b).

The upper slope connects the shelf break located close to the 130/150 m isobaths with the La Plata Terrace and is characterized by a mean slope angle of ~4–6° (Fig. 4). Independent of the width of the La Plata Terrace the upper slope has a roughly constant width of ~5–10 km reaching its maximum upslope of the Mar del Plata Canyon. The seismo-acoustic appearance of the subsurface including truncated reflections points to predominantly erosive processes, at least in the transition between the upper slope and La Plata Terrace (Fig. 4a and b).

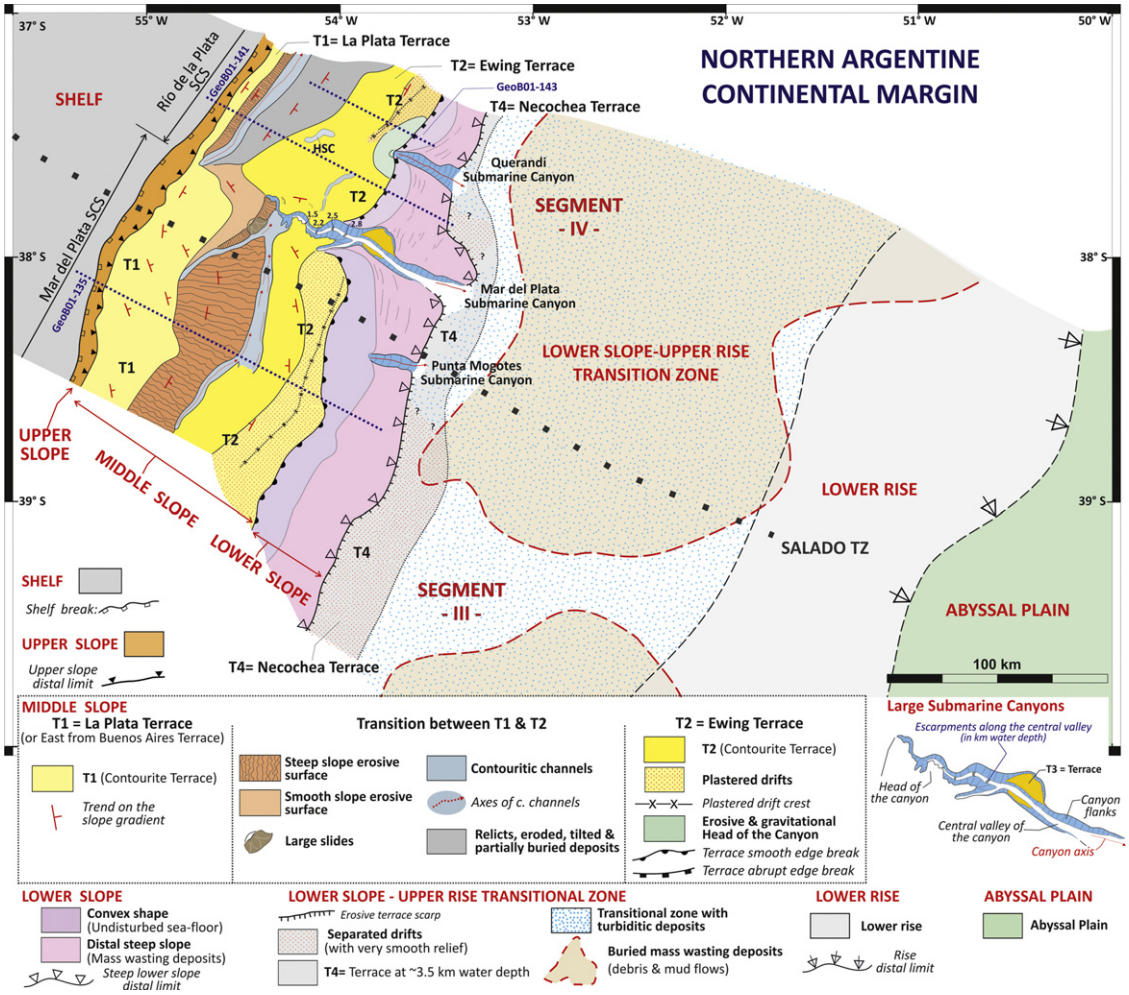

Fig. 3. Morphosedimentary map of the NE Argentine margin indicating the regional distribution of erosional, depositional, gravitational and mixed morphologies along the upper, middle, lower slope and continental rise. Seismic profiles GeoB01-135 (Fig. 4a), GeoB01-141 (Fig. 4b) and GeoB01-143 (Fig. 4c) are indicated by dashed lines. (For interpretation of the references to color in this figure legend, the reader is referred to the web version of this article.)

In the transition between the La Plata Terrace and the Ewing Terrace a mid-slope erosive surface is located (Fig. 3). Its width varies distinctly in accordance with the spatial variability of both terraces. While south of the Mar del Plata Canyon the middle slope has a mean width of ~35 km with a slope angle of 3–4°, north of the canyon the middle slope narrows to ~6 km with a slope gradient of ~6° (Figs. 3 and 4). Well-defined truncated reflections dominating the seismofacies (Figs. 4a and b, 5a and b) mark this area of the margin clearly as erosive surface.

4.2.1.2. Channels. Major slope-parallel incisions representing channels could be identified north and south of the Mar del Plata Canyon. The most prominent runs between the Ewing Terrace and the aforementioned middle slope erosive surface (Fig. 3). It follows the shape of the overall margin and is cut into the terrace building strata. In the southern area, the channel is incised ~90 m into the Ewing Terrace and reaches a width of ~5–15 km (Figs. 4a, 5b). The channel widens in the central part of the southern area, where a second contourite-parallel channel emerges from the Ewing Terrace. Another major channel runs across the margin slope at ~38°S connecting the La Plata Terrace with the major contourite channel described above (Fig. 3). It is incised 15–20 m into the margin and only 1–2 km wide.

North of the Mar del Plata Canyon the slope parallel channel is shifted landward by ~25 km and reaches a more or less constant width of ~5 km slightly widening northward with a mean depth of ~35 m (Fig. 3). At last, directly north of the Mar del Plata Canyon at ~54°W a narrow and deep contour-parallel incision ('slope-parallel channel' in Fig. 4b) was imaged, which is cut ~260 m deep into the Ewing Terrace with a maximum width of ~350 m (Fig. 3).

4.2.1.3. Minor slope-parallel incisions. In the northern part of the study area and between the Mar del Plata Canyon and the Punta Mogotes Canyon minor slope-parallel incisions (furrows) can be identified along the lower slope in water depths of ~2000–3000 m (Figs. 3, 4b and 5e). The width of the features varies between 200 and 400 m and they are ~90 m incised into the lower slope. While they are very common in the northern area, they are less abundant and of smaller dimension in the southern area ~30 km SW of the Mar del Plata Canyon (Figs. 4a and 5f).

4.2.2. Mixed erosive-depositional features—Contourite terraces

The most remarkable morphological features in the study area are the wide terraces, incised into the continental slope. There are three major terraces (Fig. 3): The La Plata Terrace (T1) and the

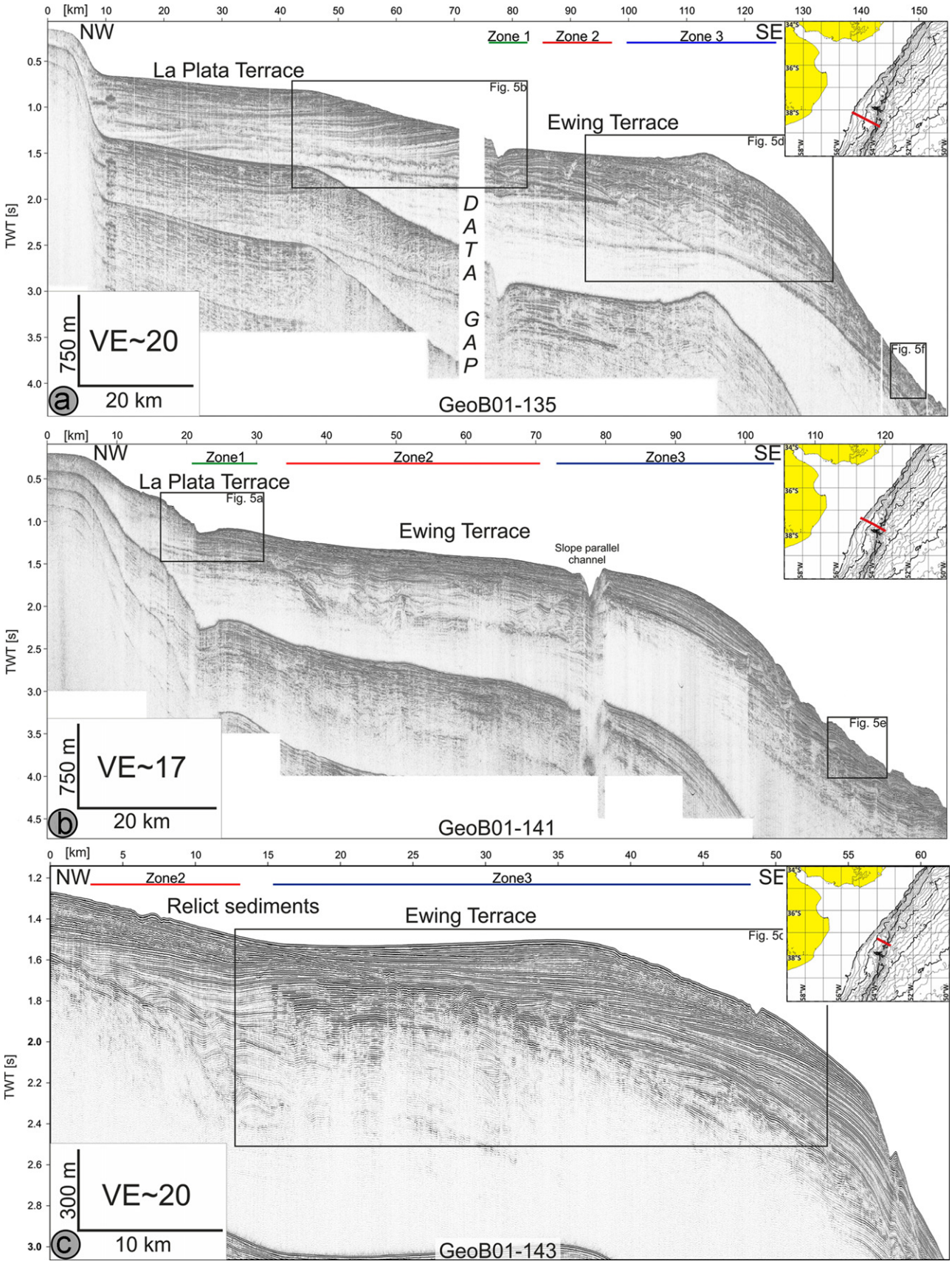

Fig. 4. High-resolution multi-channel seismic (MCS) profiles: (a) GeoB01-135 south of the Mar de Plata Canyon; (b) GeoB01-141 is directly located north of the Mar de Plata Canyon; (c) GeoB01-143 is located at the northern boundary of the study area. Both the La Plata and Ewing terraces locations are highlighted in the MCS cross sections. Locations of seismic profiles are indicated in Fig. 3. Black boxes indicate the position of close-ups shown in Fig. 5. VE ≈ vertical exaggeration.

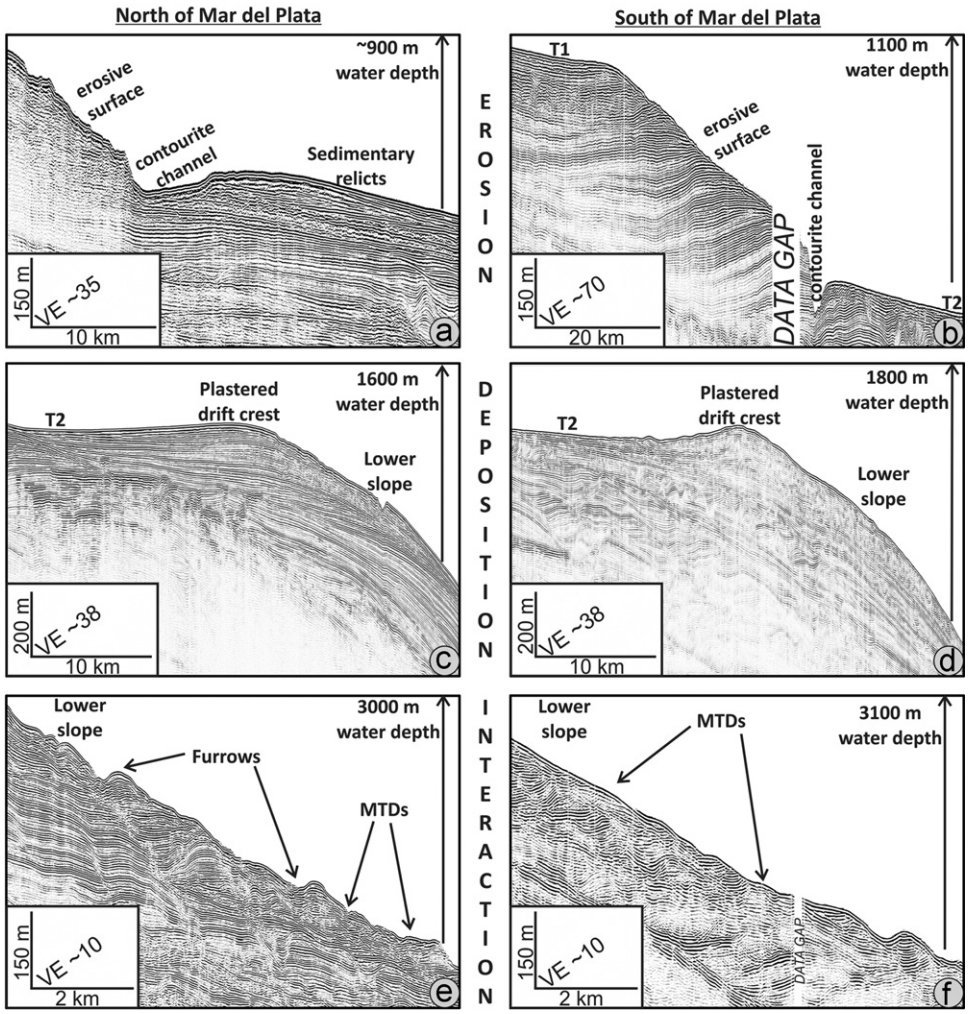

Fig. 5. Examples of morphosedimentary features for the northern and southern study area subdivided into erosive and depositional features, including an interaction of along-slope erosive and gravitational processes; T1—La Plata Terrace; T2—Ewing Terrace. See the location of the examples on Fig. 4.

Ewing Terrace (T2) on the middle slope, and the Necochea Terrace (T4) located at the foot of the slope (Fig. 4).

4.2.2.1. La Plata Terrace (T1). The shallowest terrace is the La Plata Terrace located in 500–600 m water depth with a main NE-SW orientation and a mean slope angle of 0.5–1°. The landward and seaward boundaries are marked by the upper and middle slope characterized by steeper slope angles. The terrace distinctly narrows upslope of the Mar del Plata Canyon from south (~35 km) to north (~7 km). The seismo-acoustic characteristics of the T1 strongly depend on the lateral variability of the terrace. While the terrace shows a clear horizontally layered reflection pattern of high amplitudes in the southern part of the study area (Fig. 4a), in the north the seismic facies is hard to determine due to the limited lateral extent of the terrace; only single reflections of low amplitude can be observed in this part (Fig. 4b).

4.2.2.2. Ewing Terrace (T2). The Ewing Terrace is located in water depths of 1100–1400 m and runs almost parallel to the La Plata Terrace. Characterized by a mean slope angle of ~0.5–1.5° the Ewing Terrace represents the wide area between the erosive middle slope and the lower slope (Fig. 3). This area widens from ~50 to ~80 km north of the Mar del Plata Canyon, where the upper slope is shifted landward. The Ewing Terrace can be subdivided into three zones from land to sea: Zone 1 is located at the upslope boundary of the Ewing Terrace, where truncated reflections indicate erosive processes next to the contour parallel channel described above (Figs. 4a and b, 5a and b). While this zone is quite narrow (100–150 m) in the southern part of the study area, north of the Mar del Plata Canyon this area widens to ~35 km (marked as relict sediments on Fig. 3).

Zone 2 of the terrace is characterized by nearly horizontal layered reflections (Fig. 4). Laterally, this part of the terrace drastically varies in width and shape (Fig. 3) from south (~35 km) to directly north of the Mar del Plata Canyon (~65 km). Further northward, the width of the central zone decreases.

Zone 3, located at the seaward boundary of the terrace, encompasses a major plastered drift in 1200–1400 m water depth (Figs. 3 and 4). While upslope the drift fades into the central zone, seaward deposition is terminated at the lower slope. In the center of the plastered drift a positive relief associated with a sedimentary crest can be identified (Figs. 3, 4a and c, 5c and d).

In the southern part of the study area, the 25–35 km wide elongated plastered drift with its 75 m crest covers half of the Ewing Terrace (Figs. 3 and 4a). At ~38.3°S the orientation of the crest slightly changes from a NE to a NNE trend following the general trend of the middle slope (Fig. 3). In the northern part of the study area, almost no drift deposition occurs close to the Mar del Plata Canyon. A sedimentary crest within the depositional zone can only be identified north of the Querandi canyon (Fig. 3). From there it widens northward toward the Uruguayan margin

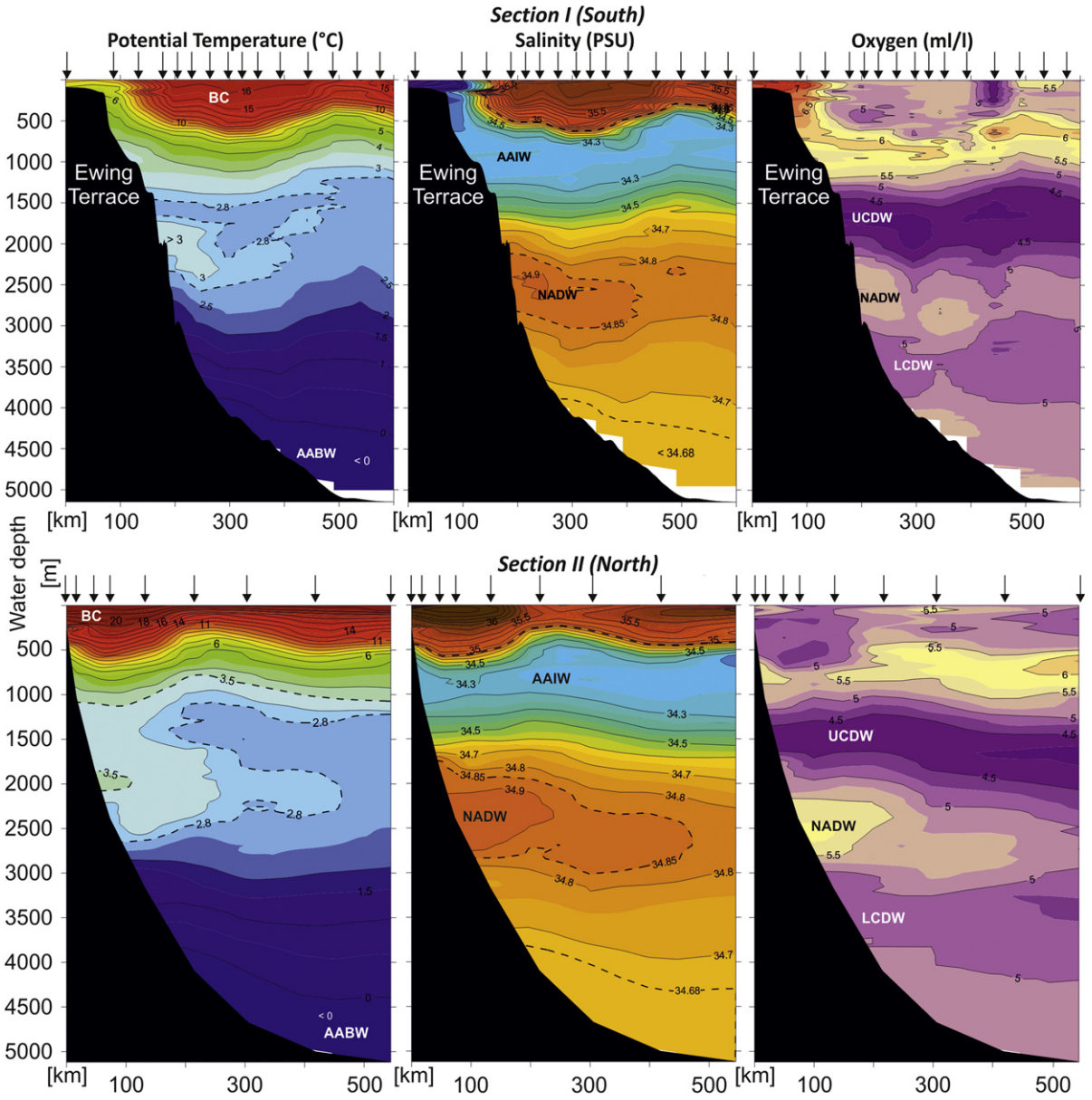

Fig. 6. Hydrographic sections (location shown in Fig. 2) of the study area showing lateral variations in potential temperature (°C), salinity and dissolved oxygen (ml/l) from the southern (Section 1, top) to the northern (Section 2, bottom) sector; BC—Brazil Current; AABW—Antarctic Bottom Water; AAIW—Antarctic Intermediate Water; LCDW—Lower Circumpolar Deep Water; NADW—North Atlantic Deep Water; UCDW—Upper Circumpolar Deep Water.

reaching a width of 30 km in the northern boundary of the study area (Figs. 4c and 5c), encompassing another plastered drift. The crest of the drift runs parallel to the middle slope and reaches a height of 35–40 m (Fig. 3).

4.2.2.3. Necochea Terrace (T4). The deepest identified terrace is the Necochea Terrace in water depths of ~3500 m (Fig. 3; Supplement 2). While landward it is limited by the lower slope, seaward the limit is hard to identify due to the gradual transition into the continental rise. In general the width of the terrace seems to vary from 5 to 35 km from north to south. Since data coverage in this deep part is sparse and only conventional, low frequency seismic images the Necochea Terrace, detailed spatial statements on the seismo-acoustic facies are not possible. However, the available data indicates an aggradational stacking pattern, representing a transition from a separated drift with very smooth relief to a plastered drift. With the given poor data coverage it seems that this depositional pattern is mostly restricted to the southern part of the study area. Only directly north of the Mar del Plata Canyon seismofacies associated with plastered drifts could be identified in a small, distinct area.

4.2.3. Gravitational features

Mass wasting deposits in the study area are mainly confined to the lower slope area and the heads and flanks of the submarine canyons (Fig. 3). As seen in Figs. 4a and b, 5e and f, gravitational processes are common on both the northern and southern lower slope in 2600–4000 ms TWT (2000–3000 m water depth) and can be identified by their chaotic seismic facies (Supplement 3). In contrast to the southern part of the study area, mass wasting deposits and their scars are more abundant and of larger dimension in the north.

Moreover, mass wasting deposits are associated to the head of the Querandi Canyon and the Punta Mogotes Canyon (Fig. 3).

4.3. Oceanographic features

4.3.1. Oceanographic Section 1—Mar del Plata Canyon

In the southern section (Section 1, Fig. 6 top) a wedge of cold (<7 °C) and fresh ($S<34.3$) Subantarctic Waters is observed in the near-surface region of the upper slope (<550 water depth). Satellite-derived sea surface temperature data reveal that this latitude marks the mean northernmost penetration of the Malvinas Current (e.g., Piola and Matano, 2001; Saraceno et al., 2004). Thus, the warm-salty and relatively low oxygen Tropical Waters and South Atlantic Central Waters carried within the BC that characterize the South Atlantic subtropical gyre are displaced offshore and are not in contact with the bottom in Section 1. Below the subtropical thermocline the salinity minimum (S_{min}) and oxygen maximum of AAIW are well defined, but near the slope they connect with the slightly warmer and less dense outer shelf waters (Fig. 6 top). At this latitude the cores of Circumpolar Deep Waters are split by the southward flowing NADW (Reid et al., 1977). The cores of these water masses along the slope are well defined in the 1200–4000 m depth range by the low–high–low salinity (34.6, >34.8, 34.75) and oxygen (<4.25, >5.25, <5 ml/l) stratification sequences (Fig. 6 top). The core of UCDW ($O_2<4.25$ ml/l) is observed at 1700 m and spans the 1500–2000 m depth range. UCDW also creates a relative potential temperature minimum matching the O_2 minimum. The high salinity core of NADW ($S>34.9$) is located at 2450 m and appears to be just separating from the slope while the NADW salinity range ($S>34.8$, Table 1) is found between 2500 and 3000 m water depths. At this location LCDW ($S<34.8$, $O_2<5$ ml/l) occupies the 3000–3900 m depth range. Below this layer, most of the abyssal ocean is covered by AABW ($\theta<0$ °C; Fig. 6 top).

4.3.2. Oceanographic Section 2—North of Mar del Plata Canyon

As expected from the general circulation patterns (Fig. 1), we find a different structure of near-bottom water masses down the slope further north (Fig. 6 bottom). The upper layer (depths less than ~500 m) is occupied by warm (>10 °C), salty ($S>35$) SACW, which flows southward associated with the Brazil Current. The salinity minimum of AAIW is clearly defined in the 700–1200 m depth range (Fig. 6 bottom). The core of AAIW in contact with the bottom along the slope is thinner than further south and displays similar salinity and slightly lower O_2 values, suggesting it is still part of a narrow northward flowing branch in contact with the slope. At Section 2 the UCDW core is still present but the oxygen minimum layer, where O_2 is less than 4.25 ml/l, is about 400 km east of the slope. Similarly, the $\theta_{min}<2.8$ °C observed in Section 1 close to the oxygen minimum is displaced offshore (Fig. 6). Consequently, in Section 2 the bulk of UCDW appears to have shifted offshore and occupies a thinner layer interacting with the bottom in the 1350–1650 m depth range (Fig. 6 bottom). The potential temperature maximum observed above the NADW maximum is not displaced vertically, but is now warmer than 3.5 °C, while the salinity maximum ($S>34.9$) has expanded vertically to the 2150–2800 m depth range. The region with $S>34.8$, our adopted definition for NADW in the Argentine Basin, spans the 1700–2900 m depth range, thus is thicker and shallower than observed further south (Fig. 6 bottom).

4.3.3. Near-bottom layers

To understand the role of the circulation and water mass structure on the described morphosedimentary features we analyzed the distribution of near-bottom (within 150 m) water mass properties based on data available in the World Ocean Database (2009) in the Argentine Basin (Fig. 7).

AAIW is confined to the upper slope, mostly between the 200 and 1000 m isobath and its northernmost location is detected at 31°S (Fig. 7). The slope narrows northward considerably and there are only two stations meeting the AAIW criteria in the narrow strip between the 200 and 1000 m isobaths in the latitude range between 34° and 31°S. North of 29°S we observe a narrow strip of AAIW along the 1000 m isobath (Fig. 7). This northern core of AAIW intersects the bottom at somewhat deeper levels than the southern core (850–1100 m), and flows as recirculated AAIW southward below the Brazil Current. The offshore limit of near-bottom UCDW closely follows the 2000 m isobath and the bulk of this water mass extends northward to about 35°S. North of 38°S there is evidence of near-bottom NADW in the depth range 1800–3000 m (Fig. 7). In the western Argentine Basin LCDW occupies a narrow near-bottom strip in the 2300–3400 m range. The interaction of LCDW with the bottom appears to extend to the southern flank of the Rio Grande Rise, and a few observations suggest isolated portions of near-bottom LCDW at depths of nearly 4000 m north of 36°S. As pointed out above, most of the bottom at depths greater than 4000 m are subjected to the influence of AABW (Fig. 7).

5. Discussion

5.1. Morphosedimentary and hydrographic features and their oceanographic and tectonic implications

5.1.1. Margin physiography

The northern Argentine margin physiography is characterized by peculiar differences in slope angle north and south of the Mar del Plata Canyon (red marks in Fig. 3). While the northern part of the study area shows a typical seaward margin inclination oblique to the upper slope, the slope south of the canyon dips northeastward and therefore, in an ~45° angle to its northern counterpart. This change in physiography might be related to the Salado Transfer Zone (STZ), which runs as well perpendicular to the upper slope in the center of the study area (Fig. 3, Supplement 1). The STZ was established during the initial opening of the South Atlantic (Hinz et al., 1999; Franke et al., 2007) and is probably characterized by non-uniform cooling of adjacent margin Segments III and IV (Allen and Allen, 1990). Periods of stronger subsidence were described associated with this structure as, e.g., during the middle Miocene (Kennett, 1982; Aceñolaza, 2000; Potter and Szatmari, 2009). Consequently, the differential tilting is presumably linked to the STZ, although its effect can mostly be observed along the La Plata Terrace (Fig. 3). Further down-slope, uniform margin inclination over the study area indicates the dominance of erosive and depositional forces, which overprint the tectonic signature.

5.1.2. Upper slope—La Plata Terrace (T1)

The La Plata Terrace is located at the upper slope in water depths between 500 and 600 m and deepens toward the north (Figs. 3 and 8). Its sedimentary style points to a uniform and continuous forcing (Figs. 5 and 6), which can only be maintained over long time periods by ocean bottom-currents, and excludes considerable downslope transport from the shelf.

Analysis of the hydrographic Section 1 (Fig. 6 bottom), which spans the La Plata Terrace, indicates that the terrace is located close to the interface between surface waters and the AAIW, which is in particular well defined in the BC by the steep thermocline in ~500 m water depth north of the Mar del Plata Canyon (Fig. 6 bottom). Such water mass interfaces, in general, represent zones dominated by turbulent, energetic current patterns driven by major vertical density gradients (Reid et al., 1977). Moreover, the high energetic

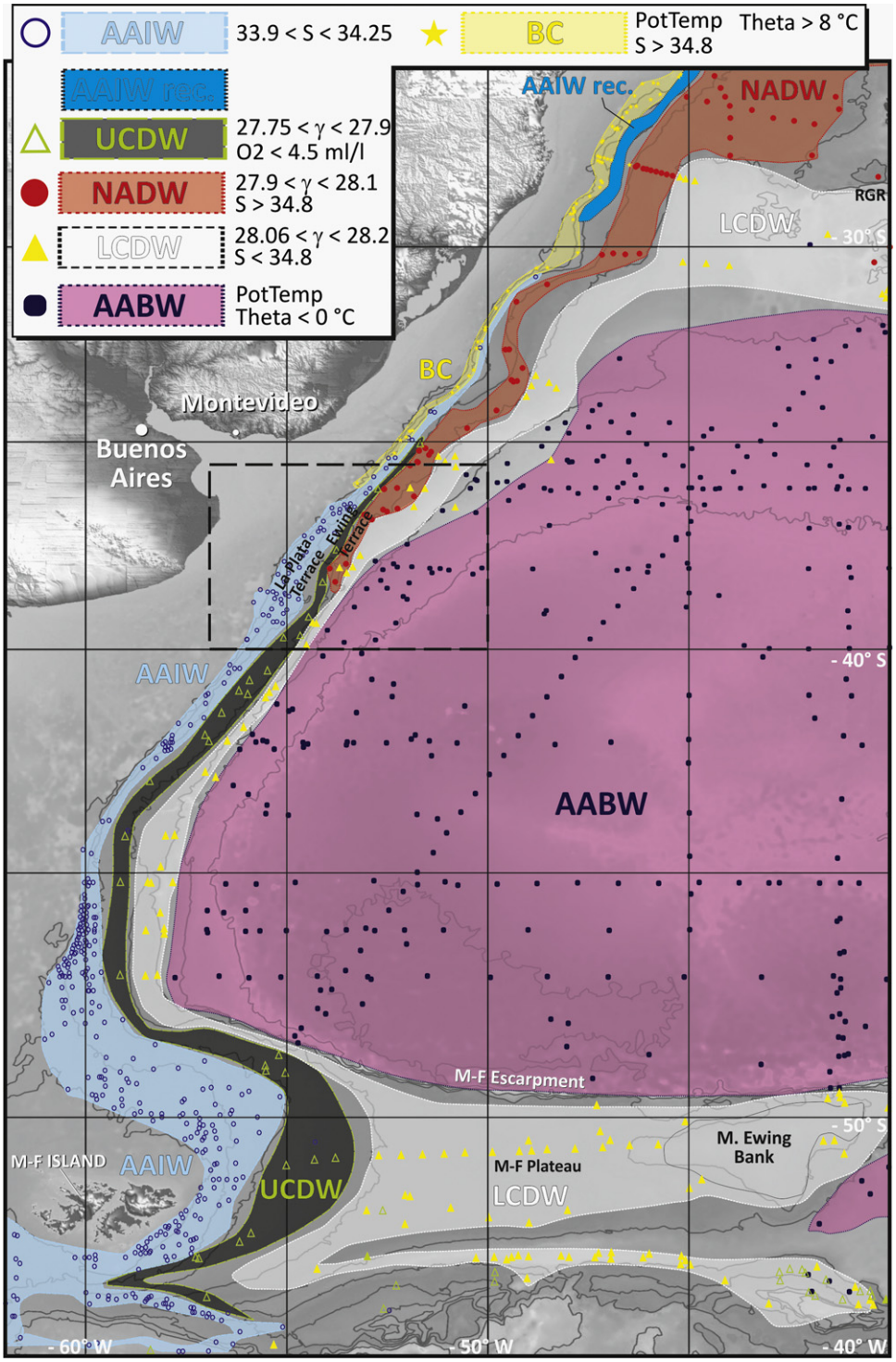

Fig. 7. Map of the Argentine Basin identifying near bottom layers depending on their physical characteristics; AABW—Antarctic Bottom Water; AAIW—Antarctic Intermediate Water; AAIW rec. —recirculated AAIW; BC—Brazil Current; LCDW—Lower Circumpolar Deep Water; M-F—Malvinas–Falkland; NADW—North Atlantic Deep Water; RGR—Rio Grande Rise; UCDW—Upper Circumpolar Deep Water; symbols identify sample location and water mass.

environment is supported by the presence of the BC and MC, which span down to the bottom along the La Plata Terrace (Fig. 7). They are in general driven by wind circulation and large lateral temperature gradients resulting in high flow velocities and contribute in this way to the high energetic environment dominating the uppermost 500–600 m of water depth.

This dynamic environment is well reflected in the sedimentary style of the slope upslope of the La Plata Terrace showing evidence of erosion (Fig. 4a and b). This remobilization of sediments is favored by the general turbulent bottom current conditions, which are locally enforced along a steep slope (McCave, 1982; McCave et al., 1982). In contrast, due to the lower slope angle terraces are characterized by more tabular flow conditions and lower flow velocities (McCave, 1982; McCave et al., 1982; Hernández-Molina et al., 2008a). Consequently, the influence of bottom-currents will result in uniform sedimentation along and across contourite terraces as shown for the La Plata Terrace (Fig. 4a). Even though current velocities are lower on top of the terrace, the dynamic current

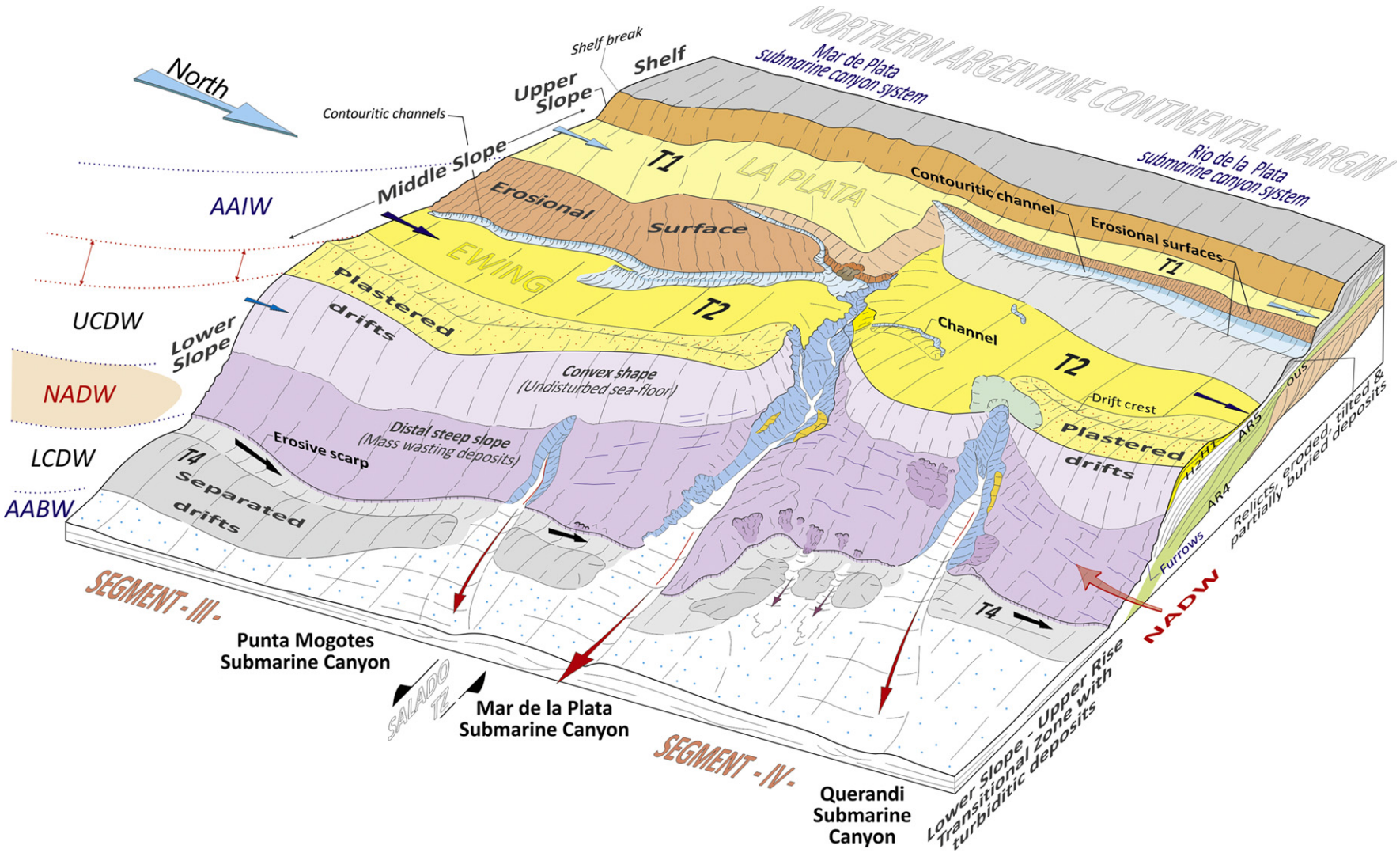

Fig. 8. 3-D map of the northern Argentine continental margin combining morphosedimentary and hydrographic features and their interpretation. Color code is consistent with Fig. 3. AABW—Antarctic Bottom Water; AAIW—Antarctic Intermediate Water; LCDW—Lower Circumpolar Deep Water; NADW—North Atlantic Deep Water; UCDW—Upper Circumpolar Deep Water.

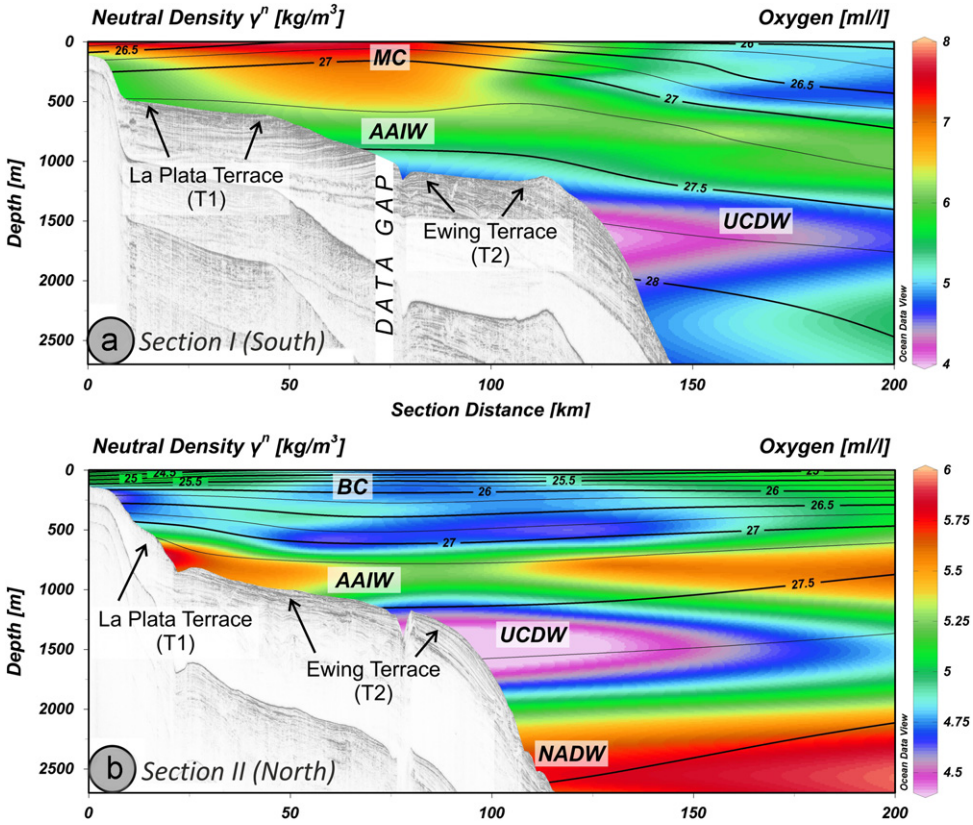

Fig. 9. Seismic–hydrographic intersections from the south (a) and north (b) of the Mar del Plata Canyon; location of seismic lines and hydrographic sections is marked in Figs. 2 and 3; seismic profiles correspond to Fig. 4a and b; color code shows oxygen content in ml/l; isopycnals are indicated by black lines; AAIW—Antarctic Intermediate Water; BC—Brazil Current; MC—Malvinas Current; (a) vertical exaggeration ~20; (b) vertical exaggeration ~17.

conditions are reflected in the deposited sediments, which show a silty to sandy character (Bozzano et al., 2011). Therefore, combining sedimentological and oceanographic evidences, we suggest that the upper slope including the La Plata Terrace and their associated sedimentary regime is strongly influenced by the surface water/AAIW interface (Figs. 8 and 9).

The high turbulent energy at this interface might be related to the presence of the BC, which due to its deep thermocline can generate large density contrasts at around 500 m depth (Fig. 6). Accordingly, the BC/AAIW interface might control sedimentary processes along the La Plata Terrace, although lateral bottom water distribution shows the offshore detachment of the BC from the margin at ~38°S (Goni et al., 2011). The southern area could in part be controlled by BC eddies, which penetrate into the MC (Piola and Matano, 2001). Single eddies allow for SACW transported within the BC to reach this region (Piola and Matano, 2001). Finally, the La Plata terrace terminates a few kilometers south of the study area (Urien and Ewing, 1974; Violante et al., 2010), as the BC does not penetrate into the MC at depth.

This circulation pattern becomes obvious comparing the northern and southern hydrographic/seismic intersections given in Fig. 9a and b. The northern section is dominated in the uppermost 500 m by waters depleted in oxygen, which represent the warm waters of the BC (Fig. 9b). In contrast, the southern section reveals high oxygen values close to the upper slope corresponding to the MC, and therefore the weaker influence of the BC (Fig. 9a).

5.1.3. Middle slope—Ewing Terrace (T2)

The largest terrace in the study area, the Ewing Terrace (Figs. 3 and 8), is located in mid-slope position in water depths of 1200–1400 m (Hernández-Molina et al., 2009; Violante et al., 2010; Krastel et al., 2011). In contrast to the La Plata Terrace, the Ewing Terrace is not a locally confined feature, but continuous along the Patagonian margin (c.f. Hernández-Molina et al., 2009), which is already indicative for a regional control of bottom-currents on the sedimentary regime.

Similar to the upper slope, there is clear evidence of ocean currents controlling sediment transport at the middle slope. Massive erosion of older strata (Fig. 4a and b, Fig. 5a and b) shapes the middle slope between the La Plata and the Ewing Terrace (Fig. 8). This erosion is related to the AAIW (Figs. 7–9), flowing as a fast bottom current favored by the margin morphology (McCave, 1982; McCave et al., 1982). This interpretation is strongly supported by approximated regional flow velocities of the OCCAM Global Ocean Model (Gwiliam et al., 1995; Gwilliam, 1996), suggesting flow velocities of ~15–20 cm/s in 1000 m water depth, which might locally increase (> 40–50 cm/s) easily in the vicinity of obstacles (e.g., changes in the slope trend, canyons heads, valleys, etc.). Such velocities allow eroding and transporting fine sand (Niño et al., 2003; McCave, 2005). Associated with the dynamic current regime and the strong erosion, measurements of high turbidity suggest the presence of intermediate nepheloid layers fed by the erosive margin processes within the AAIW.

The Ewing Terrace is located at the boundary between the AAIW and the UCDW (Figs. 3, 8 and 9). The turbulent processes associated with this water mass interface prevent sediment deposition at least over a wide area of the terrace (Zone 2 in Fig. 4). In the transition between the middle slope and the Ewing Terrace, deep contourite channels (Zone 1 in Fig. 4a and b), running parallel to the margin (Figs. 3 and 8), might indicate even the formation of helical flow patterns (cf. Hernández-Molina

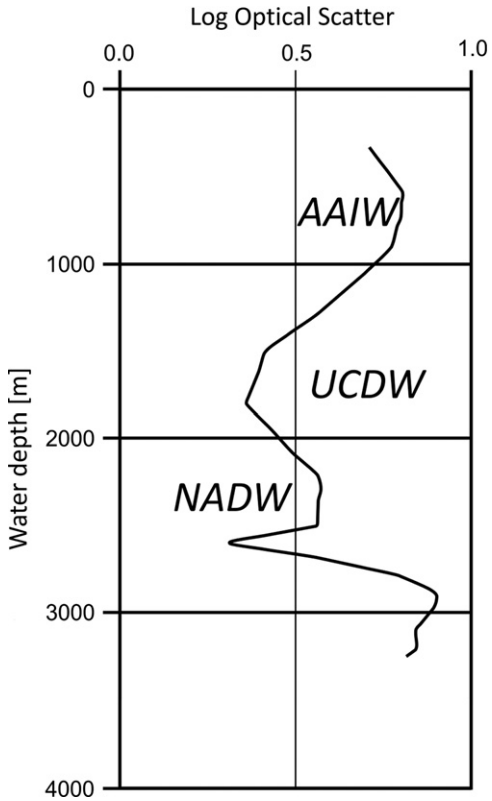

Fig. 10. Optical scatter measurements from station RC15-83 (Biscaye, 1978) with indicated water masses (AAIW—Antarctic Intermediate Water; NADW—North Atlantic Deep Water; UCDW—Upper Circumpolar Deep Water; data source: Biscaye, 1978).

et al., 2008a). The dynamics of these channels seem not be linked to the slope parallel channel in the center of the Ewing Terrace. Instead, the presence of minor faults beneath this channel (Fig. 4b) indicates a structural or gravitational control on the morphological evolution of this feature.

In contrast to the proximal area of the terrace, on its distal part plastered drift deposition occurs, indicating sedimentation focused by along-slope processes (Zone 3 in Fig. 4). Since plastered drift formation occurs under slow to intermediate flow conditions (Faugères et al., 1999), this sedimentary pattern requires a continuous decrease of flow velocities with increasing distance from the steep middle slope, which allows major parts of the upslope eroded material to deposit.

This energetic regime is reflected in the lateral variations in sedimentary characteristics across the terrace. While in the transition from the upper slope erosive features are located close to the helical flow pattern, the central area of the terrace is characterized by non-deposition or low sedimentation, as suggested by the narrow spacing of horizontal reflectors (Fig. 4). In turn, at the seaward limit of the Ewing Terrace the plastered drift sequences indicate the lowest current velocities. This interpretation is supported by sedimentological data showing a gradient from gravel rich contourite material located in the contourite channel to more silty material at the drift's crest (Bozzano et al., 2011). Additionally, this scenario as well fits to the observed turbidity values (Fig. 10). Within the AAIW suspended particle load is highest, reflecting ongoing erosion of sediments along the middle slope. The amount of suspended sediments decreases drastically towards the UCDW, not only indicating the lower transport capacity of the UCDW, but as well supporting the formation of a plastered drift through lower energy conditions.

The described conditions at the depth of the terrace are probably significantly enhanced during glacial times, when the AAIW/UCDW interface is shifted upward (Preu et al., 2012) and the turbulent energy of the interface is superseded by calmer conditions characterizing the UCDW. However, the overall sedimentary configuration of the Ewing Terrace indicates that even during glacial times the steep slope allows for strong enough current velocities to prevent sedimentation on the seaward half of the terrace.

The most prominent change in slope morphology within the study area is represented by the narrowing of the middle slope in close vicinity to the Mar del Plata Canyon and the associated change in the depositional style (Figs. 3 and 8). One possible explanation might be offered by the BMC, which might strongly influence the ocean circulation in greater depth (Preu et al., 2012). The detachment of NADW from the northern Argentine margin (Reid et al., 1977), which is associated with the BMC, has a major effect on vertical water mass stratification (Georgi, 1981; Saunders and King, 1995; Piola and Matano, 2001; Carter and Cortese, 2009), and therefore on the position of water mass interfaces in the study area (cf. Fig. 9a and b). In addition, in this area AAIW flowing northward along with the MC impinges recirculated AAIW flowing southward (Piola and Matano, 2001). The resulting high energetic mixing could be hold responsible for the stronger erosion and the associated cutting-back of the middle slope north of the Mar del Plata Canyon resulting in significantly higher slope gradients in comparison to the southern area (Fig. 5a and b). Furthermore, this pattern would be strengthened by deep-reaching eddies traveling within the BC, which would also pass through the BMC. Such eddies are known to influence sedimentary processes even in great depth (Hollister and McCave, 1984; Hollister, 1993) and are capable to erode and transport vast amounts of sediments (Viana and Faugères, 1998) or even shape large-scale terraces as e.g., off SE Africa (Preu et al., 2011). At last, internal waves originating from the fast flowing, turbulent oceanographic regime associated with the BMC might represent an important controlling factor. These energetic patterns are known to influence sedimentary processes and might result in massive sediment resuspension (Puig et al., 2004; Pomar et al., 2012). Consequently, we propose that the lateral variations in width of the Ewing Terrace are the result of the massive forces associated with the BMC. However, partly structural control on the distinct northward constriction of the La Plata Terrace and the middle slope cannot be excluded completely due to the presence of the Salado Transfer Zone (STZ), although satellite-derived gravity measurements (Smith and Sandwell, 1997) determined its position south of this major physiographic change (Franke et al., 2007).

The change in depositional style along the Ewing Terrace in close vicinity of the Mar del Plata Canyon cannot be explained by the large-scale ocean circulation. Whether the canyon or the overall change in margin physiography disturbs the sedimentary processes forming the plastered drift will be determined in future studies (c.f. Preu, 2011).

5.1.4. *Lower slope—Furrows and the Necochea Terrace (T4)*

The shape of the lower slope differs from the previously described and discussed shapes of the upper and middle slope. Figs. 3 and 8 indicate the smooth and regular margin shape in water depths between 1500 and 2000 m, which is only disturbed by the presence of the Mar del Plata and Querandi canyons cutting into the plastered drift strata. This part of the margin is under the influence of the UCDW (Figs. 7–9), which flows with relatively low velocities along the northern Argentine margin as suggested by low turbidity values (Fig. 10) and consequently favors drift deposition (Fig. 5c and d).

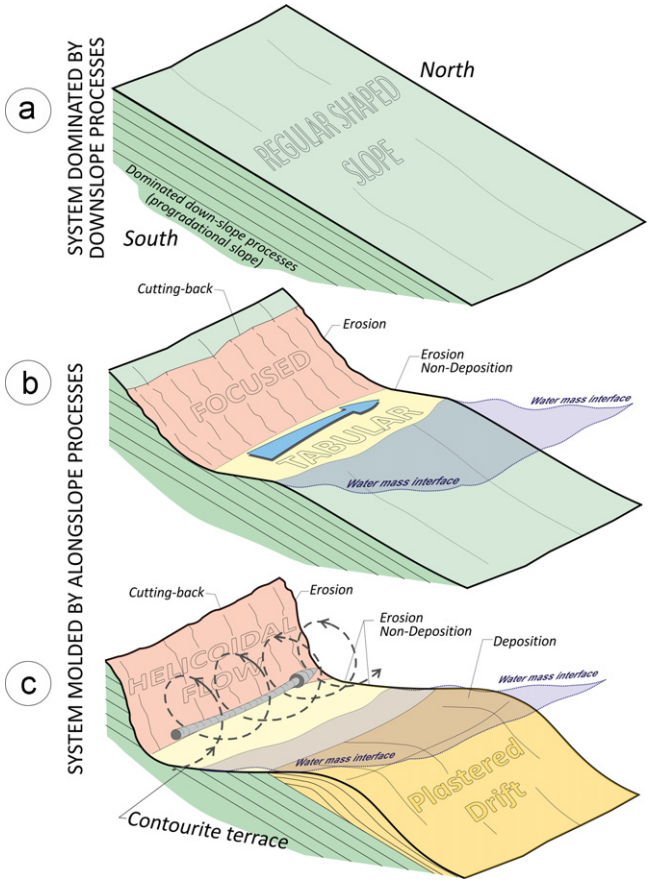

Fig. 11. Schematic model for the southern hemisphere (without scale) explaining contourite terrace formation considering erosive processes associated to water mass boundaries. These interfaces force the system to progress from a down-slope process dominated stage (a) to a stage molded by along-slope processes ((b) and (c)).

In ~2000 m water depth not only the gradient of the lower slope changes, but also the margin morphology (Figs. 3 and 8). The hummocky surface of the lower slope indicates down-slope processes as indicated by sediment echosounder data (Supplement 3). These are probably associated with the upslope drifts building the Ewing Terrace since the middle Miocene (Hernández-Molina et al., 2009; Preu et al., 2012), which are susceptible to failure due to locally focused sedimentation (Laberg et al., 2008.

The minor slope-parallel incisions represent furrows, which are mainly located along the scars of the former sediment failures (Figs. 4b, and 5e) and suggest the influence of erosive bottom currents (Viana, 2008). Consequently, the abundance of furrows in water depth between 2000 and 3000 m points toward the NADW, flowing as erosive bottom current (Fig. 8). The link to the NADW as margin shaping current is strengthened by turbidity observations, which show relative maxima in the corresponding water depths (Fig. 10). Therefore, the absence of the furrows south of the canyon (Figs. 4a and 5f) would be the result of detaching NADW from the Argentine margin (Fig. 9) As a result, we propose that the furrows are linked to the presence of the NADW, which would be locally focused due to seafloor irregularities and minor incisions created by gravitational processes.

In water depths of ~3500 m, the Necochea Terrace (T4) shapes the margin (Figs. 3 and 8, Supplement 2). The prograding character of strata indicates the influence of the surrounding oceanographic regime. Fig. 6 shows clearly that the Necochea Terrace is today under the control of the LCDW core. Similar terraces were described for the southern Argentine margin (Valentin Feilberg Terrace), which are as well connected to Southern Ocean sources of deep water masses (Hernández-Molina et al., 2009, 2010).

The variations in the sedimentary pattern from north to south might be linked to the variations in the NADW pattern, since as a result of detaching NADW from the margin the flow behavior of the LCDW probably also changes. Confined in space by the NADW, the LCDW flows faster north of the Mar del Plata Canyon prohibiting sediment deposition. In contrast, south of the canyon the drift formation is possible due to lower current activity. However, this concept of long-term behavior is in conflict with the recent hydrographic data (Figs. 6 and 7), which suggest no significant changes in the LCDW and AABW cores within the study area. This controversy might result from the joint interpretation of results being representative for short (hydrographic data) and extensive (geological data) periods of time.

An exception from the depositional pattern marks the area directly north of the Mar del Plata Canyon exit in the centre of the study area. Exceptionally high sediment accumulation occurs in the current lee side, hence supporting the hypothesis that the controlling water mass flows northward (Figs. 3 and 8).

5.2. Genesis of contourite terraces

5.2.1. General concept

Based on our data collection, we propose a concept of formation of contourite terraces by the interplay between margin physiography and the local bottom current regime (Fig. 11). Water mass interfaces and their associated turbulent energy patterns might result in erosion along regular shaped margins (Fig. 11a). This energetic pattern is enforced by internal tides and internal waves, which have a tremendous effect on sediment dynamics and result in erosion and resuspension (Dickson and McCave, 1986; van Raaphorst et al., 2001; Bonnin et al., 2002; Cacchione et al., 2002; Hosegood and van Haren, 2003). Once the regular margin shape has changed, upslope the slope steepens, while a smaller terrace-like feature developed along the water mass interface (Fig. 11b).

The terrace itself will strongly influence the local flow pattern due to its shape. McCave (1982) described the relation between slope gradient and potential flow velocities in a case study at the Bermuda Rise suggesting that steeper slopes favor higher current velocities and in consequence lead to erosive processes. In contrast, terrace-like morphologies would result in calmer and more tabular flow conditions. Accordingly, a terrace would be characterized either by a uniform depositional style or, as the case may be, on extensive terraces by lateral variation from non-deposition to drift formation. While this depositional pattern would preserve the overall terrace shape, the upslope connected slope would concurrently be eroded due to locally increased current velocities. The erosion might be in particular enforced in scenarios, where the ocean currents are deflected towards the margin by the Coriolis force (Faugères and Mulder, 2011). On geological time scales the combination of both processes will lead to a cutting-back of the slope and a widening of the terrace (Fig. 11b).

Depending on the overall flow velocities and sediment properties, the locally confined velocity maximum might lead to enhanced erosion forming a contour channel at the transition between the steep slope and the terrace (Fig. 11c). Therefore, a helical flow pattern can evolve, which in turn continuously deepens the channel due to enforced erosive processes. The eroded and resuspended material provided by these processes is transported along the terrace. Once the terrace reaches a certain extent drift formation at the seaward limit becomes possible (Fig. 11c; Faugères and Mulder, 2011) and results in sedimentary patterns similar to slope-parallel contouritic mounded

deposits following the depositional concepts introduced in Faugères et al. (1999).

This model does not require structural control on the original formation of terraces. However, since terraces might as well be predetermined by tectonic processes, a tectonic origin must be ruled out to explain their evolution exclusively from bottom current activity. Once the terrace was already formed, in both cases sedimentary processes would be similar to the above described (Fig. 11b and c).

5.2.2. Contourite terraces along the northern Argentine margin

Since structural control on terrace formation can be excluded for the northern Argentine margin based on deep reaching multichannel seismic data (Hinz et al., 1999), the evolution of contourite terraces is most probably related to oceanographic processes.

Considering the above described deep thermocline associated to the BC/AAIW interface (Figs. 6 and 7), the origin of the La Plata Terrace can be linked to water mass interface related processes (Fig. 8). Since changes in temperature go along with changes in density, the BC/AAIW interface is particular susceptible for internal wave generation and propagation, which are capable to initiate or enforce erosive processes (Fig. 9a).

These high energetic patterns might not only influence the La Plata Terrace but the Ewing Terrace as well. Since the Ewing Terrace correlates with the AAIW/UCDW interface (Fig. 9), which represents a convenient surface to reflect and focus internal wave energy, the initial evolution of the Ewing Terrace might as well be related to processes in shallower water. Additionally, several studies suggested that the Ewing Terrace is controlled by the AAIW/UCDW interface since the middle Miocene (Hernández-Molina et al., 2009; Violante et al., 2010; Preu et al., 2012). These studies not only suggest a cutting of the terrace into former strata but also a widening of the Ewing Terrace due to drift deposition at the seaward limit of the terrace (Fig. 11c).

Since the Necochea Terrace is located within the LCDW, its position along the slope seems to exclude the water mass interface model (Fig. 6). However, this is not completely true considering that terrace formation is a process acting on longer geological times. During glacial times for example, the overall influence of Antarctic water masses on the southern hemisphere increases (Duplessy et al., 1988; Mulitza et al., 2007). This includes probably an increase in AABW production (Ninnemann and Charles, 2002; Piotrowski et al., 2008), which is still under debate (e.g., Curry and Lohmann, 1982; Weber et al., 1994; Krueger et al., 2012). An overall strengthened influence of southern sourced water will lead to a thickening of the AABW layer at the Argentine margin. In contrast, NADW production is strongly reduced during cold periods (Oppo and Fairbanks, 1987; McCave et al., 1995; Rasmussen et al., 1996; Venz et al., 1999; Knutz, 2008), which leads to a thinning of the NADW layer in the SW Atlantic (Kennett, 1982; Viana et al., 2002; Preu et al., 2012). While the thickening of the AABW displaces the LCDW/AABW-interface upward, there is no counterforce given by the NADW, which influence is significantly reduced. This scenario would place the LCDW/AABW interface close to the Necochea Terrace during glacial times and therefore suggest that the terrace formation processes are mainly active during cold periods in this part of the margin. Consequently, the forcing responsible for the development of the Necochea Terrace would be highly variable on geological timescales, which is reflected by its limited extent on the margin.

5.3. Implications on the position of the BMC on geological time scales

Linking of lateral variations in terrace morphology and the associated erosive features to the regional oceanography (Figs. 8 and 9) allow not only terrace formation processes, but also the history of the controlling oceanic regime to be reconstructed. This is in particular valid for the dynamics of the BMC, which marks the southernmost influence of the BC and the NADW along the Argentine margin.

The lateral continuity and shape of the La Plata Terrace is strongly bound to variations in the BC flow pattern. Since the La Plata terrace terminates a few kilometers south of the study area (Urien and Ewing, 1974), this scenario would suggest that the modern situation of the BMC would be close to its southernmost position on geological time scales. This might be at least valid for Quaternary times, when climate is dominated by glacial/interglacial cycles. While the modern position of the BMC would mark the location during interglacials, the BMC was probably shifted northward due to a stronger influence of southern-sourced waters during glacials (Duplessy et al., 1988; Mulitza et al., 2007; Preu et al., 2012). This northward migration of the BMC can be shown by its seasonal variation on much shorter time scale. Seasonal variability of the BMC (Supplement 4) derived from satellite observations (Saraceno et al., 2004) show a northward migration from southern hemisphere summer to winter. This interpretation is in agreement with the location of the seasonal frontal probability maxima, which was derived from very high-resolution radiometer data (Saraceno et al., 2004). Following this concept, the position of the BMC would be located further northward during cold periods.

This interpretation is supported by the appearance of furrows at the lower slope mainly in the northern part of the study area (Figs. 3, 4b, 5f and 8). These features are probably produced by the interaction of NADW with the hummocky seafloor topography, which is the result of mass wasting processes. The southern limit of the NADW is marked by the location of the BMC, as well, where it is deflected and loses its margin constraint (Piola and Matano, 2001). Therefore, the noticeable disappearance of these slope parallel incisions toward the south indicates the southernmost influence of the NADW, and in turn of the BMC on geological timescales.

6. Conclusion

Morphosedimentary analysis of the northern Argentine margin based on seismo-acoustic and hydro-acoustic data were used to characterize erosive and depositional features including mass transport deposits and their lateral variability. Three major terraces were described located in 500–600 m (La Plata Terrace), 1100–1400 m (Ewing Terrace) and 3500 m (Necochea Terrace) water depth, respectively. The two shallowest are connected upslope to particularly steep erosional slopes. The margin shape distinctly changes in the center of the study area close to the Mar del Plata Submarine Canyon. While the La Plata Terrace narrows from south to north, the Ewing Terrace widens.

Correlation of the morphosedimentary features with the regional oceanographic regime revealed a pronounced correlation between depths of the terraces and the depths of the water masses interfaces. While the La Plata Terrace reflects the Brazil Current/Antarctic Intermediate Water interface, the Ewing Terrace is located at the Antarctic Intermediate Water/Upper Circumpolar Deep Water transition. The Necochea Terrace was probably located at the Lower Circumpolar Deep Water/Antarctic Bottom Water interface during glacial times.

The presence of these terraces along water mass interfaces suggests turbulent energy associated to these zones as initial mechanism for terrace formation. Once the first smaller incision is carved into the margin, the currents will be enforced along the steeper segments of the slope. Calmer, tabular conditions will dominate on the seaward parts the terraces. The combination of both flow patterns results in a cutting-back of the margin. Through

time the terrace may reach a size that the seaward boundary of the terrace is outside of the high velocity zone acting at the steeper parts of the slope, supporting then contourite drift deposition.

Since the lateral variability of erosive features depends strongly on the surrounding oceanographic regime, our data indicates that the Brazil–Malvinas Confluence was located in its modern position or further northward during Quaternary times.

This study represents a clear example for synergies derived from an interdisciplinary approach combining geological, geophysical and oceanographic data sets for characterization of depositional and erosive features related to alongslope processes on a, what we think, type location for current-influenced continental margins. Consequently, the depositional and erosive features described here may serve as a guideline for future studies to identify reliable oceanographic indicators, being useful also for studies on regional ocean circulation in oceanography.

Acknowledgements

The study was funded through DFG-Research Center/ Cluster of Excellence "The Ocean in the Earth System" and was supported by the Bremen International Graduate School for Marine Sciences (GLOMAR) that is funded by the German Research Foundation (DFG) within the frame of the Excellence Initiative by the German federal and state governments to promote science and research at German universities.

The study is related to the CONTOURIBER project (CTM 2008-06399-C04/MAR) and MOWER projects (CTM 2012-39599-C03). Further this study is associated to the PICT 2010-0953 project from the Argentine Ministry of Science and Technology and the IGCP project 619 (Contourites: geological record of ocean-driven paleoclimate, accomplice of submarine landslides and reservoir of marine geo-resources). Additional support was given by the Inter-American Institute for Global Change Research (IAI) CRN 2076 which is supported by the US National Science Foundation (Grant GEO-0452325).

Acoustic data were processed using 'Vista 2D/3D Seismic Processing', which is a registered trademark of GEDCO. Seismic interpretation and images were undertaken using 'Seismic Micro-Technology KINGDOM Advanced'.

The authors particularly thank the participants of an Argentine Margin Workshop held at MARUM in January, 2011, including Dr. D.A.W. Stow (Heriot-Watt Univ., Edinburgh, UK) for fruitful discussions and support during the improvement of this manuscript. Constructive comments by an anonymous referees and the editor significantly improved the quality of this manuscript.

We like to thank Captain Kull, Captain Baschek and the crew of R/V Meteor cruises M49/2 and M78/3 for their excellent work and support.

Appendix A. Supplementary materials

Supplementary data associated with this article can be found in the online version at http://dx.doi.org/10.1016/j.dsr.2012.12.013.

References

Aceñolaza, F.G., 2000. La Formación Paraná (Mioceno medio): estratigrafía, distribución regional y unidades equivalentes. In: Aceñolaza, F.G., Herbst, R. (Eds.), El Neógeno de Argentina. INSUGEO, Tucumán, Argentina, pp. 9–27.

Allen, P., Allen, J., 1990. Basin Analysis. Blackwell Publishing, Malden.

Anonymous, 1992, South Atlantic Ventilation Experiment (SAVE), Chemical, Physical and CTD Data Report. Scripps Institution of Oceanography, Oceanographic Data Facility. ODF Publication 232, SIO Reference 92-10, 625 pp.

Arhan, M., Carton, X., Piola, A., Zenk, W., 2002. Deep lenses of circumpolar water in the Argentine Basin. J. Geophys. Res. 107 (C1), 3007, http://dx.doi.org/10.1029/2001jc000963.

Arhan, M., Mercier, H., Park, Y.-H., 2003. On the deep water circulation of the eastern South Atlantic Ocean. Deep Sea Res. Part I 50 (7), 889–916.

Biscaye, P.E., 1978. Nepheloid Layer Composition. 〈http://www.geomapapp.org/database/neph_data/RC15/RC15-083.txt〉.

Bonnin, J., van Raaphorst, W., Brummer, G., van Haren, H., Malschaert, H., 2002. Intense mid-slope resuspension of particulate matter in the Faeroe–Shetland Channel: short-term deployment of near-bottom sediment traps. Deep Sea Res. Part I 49 (8), 1485–1505, http://dx.doi.org/10.1016/s0967-0637(02)00030-4.

Bozzano, G., Violante, R., Cerredo, M.E., 2011. Middle slope contourite deposits and associated sedimentary facies off NE Argentina. Geo-Mar. Lett. 31 (5–6), 495–507, http://dx.doi.org/10.1007/s00367-011-0239-x.

Cacchione, D.A., Pratson, L.F., Ogston, A.S., 2002. The shaping of continental slopes by internal tides. Science 296 (5568), 724–727, http://dx.doi.org/10.1126/science.1069803.

Camp, D., Haines, W., Huber, B., 1985. Marathon Leg 7 R/V Thomas Washington CTD/Hydrographic Data. Preliminary Report. Lamont-Doherty Geol. Observ..

Carter, L., Cortese, G., 2009. Change in the Southern Ocean: responding to Antarctica. In: Brigham-Grette, J., Powell, R., Newman, L., Kiefer, T. (Eds.), PAGES News: Change at the Poles, a Paleoscience Perspective. PAGES International Project Office, pp. 30–32.

Casey, K.S., Cornillon, P., 1999. A comparison of satellite and in situ–based sea surface temperature climatologies. J. Climate 12 (6), 1848–1863, http://dx.doi.org/10.1175/1520-0442(1999)012 < 1848:acosai > 2.0.co;2.

Chelton, D.B., Schlax, M.G., Witter, D.L., Richman, J.G., 1990. Geosat Altimeter observations of the surface circulation of the Southern Ocean. J. Geophys. Res. 95 (C10), 17877–17903.

Curry, W.B., Lohmann, G.P., 1982. Carbon isotopic changes in benthic foraminifera from the western South Atlantic: Reconstruction of glacial abyssal circulation patterns. Quat. Res. 18 (2), 218–235, http://dx.doi.org/10.1016/0033-5894(82)90071-0.

Dickson, R.R., McCave, I.N., 1986. Nepheloid layers on the continental slope west of Porcupine Bank. Deep Sea Res. Part A 33 (6), 791–818, http://dx.doi.org/10.1016/0198-0149(86)90089-0.

Duarte, C.S.L, Viana, A.R., 2007. Santos Drift System: stratigraphic organization and implications for late Cenozoic palaeocirculation in the Santos Basin, SW Atlantic Ocean. In: Viana, A.R., Rebesco, M. (Eds.), Economic and Palaeoceanographic Significance of Contourite Deposits, 276. Geological Society, London, pp. 171–198, Special Publications.

Duplessy, J.C., Shackleton, N.J., Fairbanks, R.G., Labeyrie, L., Oppo, D., Kallel, N., 1988. Deepwater source variations during the last climatic cycle and their impact on the global deepwater circulation. Paleoceanography 3 (3), 343–360.

Ewing, M., Lonardi, A.G., 1971. Sediment transport and distribution in the Argentine Basin. 5. Sedimentary structure of the Argentine margin, basin, and related provinces. Phys. Chem. Earth 8, 123–251.

Faugères, J.C., Mézerais, M.L., Stow, D.A.V., 1993. Contourite drift types and their distribution in the North and South Atlantic Ocean basins. Sediment. Geol. 82 (1–4), 189–203.

Faugères, J.C., Mulder, T., 2011. Contour currents and contourite drifts. In: Huneke, H., Mulder, T. (Eds.), Developments in Sedimentology. Elsevier, Amsterdam, pp. 149–214.

Faugères, J.-C., Stow, D.A.V., Imbert, P., Viana, A., 1999. Seismic features diagnostic of contourite drifts. Mar. Geol. 162 (1), 1–38.

Flood, R.D., Shor, A.N., 1988. Mud waves in the Argentine Basin and their relationship to regional bottom circulation patterns. Deep Sea Res. Part A 35 (6), 943–971, http://dx.doi.org/10.1016/0198-0149(88)90070-2.

Franke, D., Neben, S., Ladage, S., Schreckenberger, B., Hinz, K., 2007. Margin segmentation and volcano-tectonic architecture along the volcanic margin off Argentina/Uruguay, South Atlantic. Mar. Geol. 244 (1–4), 46–67, http://dx.doi.org/10.1016/j.margeo.2007.06.009.

García, M., Hernández-Molina, F.J., Llave, E., Stow, D.A.V., León, R., Fernández-Puga, M.C., Diaz del Río, V., Somoza, L., 2009. Contourite erosive features caused by the Mediterranean Outflow Water in the Gulf of Cadiz: quaternary tectonic and oceanographic implications. Mar. Geol. 257 (1–4), 24–40, http://dx.doi.org/10.1016/j.margeo.2008.10.009.

Georgi, D.T., 1981. On the relationship between large-scale property variations and finestructure in the Circumpolar Deep Water. J. Geophys. Res. 86, 6556–6566.

Goni, G.J., Bringas, F., DiNezio, P.N., 2011. Observed low frequency variability of the Brazil Current front. J. Geophys. Res. 116, C10037, http://dx.doi.org/10.1029/2011JC007198.

Gruetzner, J., Uenzelmann-Neben, G., Franke, D., 2012. Variations in sediment transport at the central Argentine continental margin during the Cenozoic. Geochem. Geophys. Geosyst. 13 (1–15), Q10003, http://dx.doi.org/10.1029/2012GC004266.

Gwilliam, C.S., 1996. Modelling the global ocean circulation on the T3D. In: Ecer, A., Periaux, J., Satdfuka, N., TaylorA2 – A, S., Ecer, J.P.N.S., Taylor, S. (Eds.), Parallel Computational Fluid Dynamics 1995. North-Holland, Amsterdam, pp. 33–40.

Gwiliam, C.S., Coward, A.C., de Cuevas, B.A., Webb, D.J., Rourke, E., Thompson, S.R., Döös, K., 1995. The OCCAM Global Model. In: Second UNAM-Cray Supercomputing Conference on Numerical Simulations in the Envionmental and Earth Sciences.

Heezen, B.C., 1959. Dynamic processes of abyssal sedimentation: erosion, transportation, and redeposition on the deep-sea floor. Geophys. J. R. Astron. Soc. 2 (2), 142–172, http://dx.doi.org/10.1111/j.1365-246X.1959.tb05790.x.

Heezen, B.C., Hollister, C., 1964. Deep-sea current evidence from abyssal sediments. Mar. Geol. 1 (2), 141–174, http://dx.doi.org/10.1016/0025-3227(64)90012-X.

Henkel, S., Strasser, M., Schwenk, T., Hanebuth, T.J.J., Hüsener, J., Arnold, G.L., Winkelmann, D., Formolo, M., Tomasini, J., Krastel, S., Kasten, S., 2011. An interdisciplinary investigation of a recent submarine mass transport deposit at the continental margin off Uruguay. Geochem. Geophys. Geosyst. 12 (8), Q08009, http://dx.doi.org/10.1029/2011gc003669.

Hernández-Molina, F.J., Llave, E., Somoza, L., Fernández-Puga, M.C., Maestro, A., León, R., Medialdea, T., Barnolas, A., García, M., del Río, V.D., Fernández-Salas, L.M., Vázquez, J.T., Lobo, F., Dias, J.M.A., Rodero, J., Gardner, J., 2003. Looking for clues to paleoceanographic imprints: a diagnosis of the Gulf of Cadiz contourite depositional systems. Geology 31 (1), 19–22, http://dx.doi.org/10.1130/0091-7613(2003)031<0019:lfctpi>2.0.co;2.

Hernández-Molina, F.J., Llave, E., Stow, D.A.V., 2008a. Continental slope contourites. Developments in sedimentology.. In: Rebesco, M., Camerlenghi, A. (Eds.), Contourites. Elsevier, pp. 379–408 2008.

Hernández-Molina, F.J., Maldonado, A., Stow, D.A.V., Rebesco, M., Camerlenghi, A., 2008b. Abyssal plain contourites. Developments in sedimentology.. In: Rebesco, M., Camerlenghi, A. (Eds.), Contourites. Elsevier, pp. 345 347–378, 2008.

Hernández-Molina, F.J., Paterlini, M., Somoza, L., Violante, R., Arecco, M.A., de Isasi, M., Rebesco, M., Uenzelmann-Neben, G., Neben, S., Marshall, P., 2010. Giant mounded drifts in the Argentine continental margin: origins, and global implications for the history of thermohaline circulation. Mar. Pet. Geol. 27 (7), 1508–1530, http://dx.doi.org/10.1016/j.marpetgeo.2010.04.003.

Hernández-Molina, F.J., Paterlini, M., Violante, R., Marshall, P., de Isasi, M., Somoza, L., Rebesco, M., 2009. Contourite depositional system on the Argentine slope: an exceptional record of the influence of Antarctic water masses. Geology 37 (6), 507–510, http://dx.doi.org/10.1130/g25578a.1.

Hernández-Molina, F.J., Preu, B., Violante, R.A., Piola, A.R., Paterlini, C.M., 2011. Las terrazas contorníticas en el Margen Continental Argentino: implicaciones morfosedimentarias y oceanográficas. Geogaceta 50–52, 145–148.

Hinz, K., Neben, S., Schreckenberger, B., Roeser, H.A., Block, M., Souza, K.G.d., Meyer, H., 1999. The Argentine continental margin north of 48°S: sedimentary successions, volcanic activity during breakup. Mar. Pet. Geol. 16 (1), 1–25.

Hollister, C.D., 1993. The concept of deep-sea contourites. Sediment. Geol. 82 (1–4), 5–11.

Hollister, C.D., McCave, I.N., 1984. Sedimentation under deep-sea storms. Nature 309 (5965), 220–225, http://dx.doi.org/10.1038/309220a0.

Hosegood, P., van Haren, H., 2003. Ekman-induced turbulence over the continental slope in the Faeroe–Shetland Channel as inferred from spikes in current meter observations. Deep Sea Res. Part I 50 (5), 657–680, http://dx.doi.org/10.1016/s0967-0637(03)00038-4.

Kennett, J., 1982. Marine Geology. Prentice Hall, New Jersey.

Klaus, A., Ledbetter, M.T., 1988. Deep-sea sedimentary processes in the Argentine Basin revealed by high-resolution seismic records (3.5 kHz echograms). Deep Sea Res. Part A 35 (6), 899–917, http://dx.doi.org/10.1016/0198-0149(88)90067-2.

Knutz, P.C., 2008. Palaeoceanographic significance of contourite drifts. In: Rebesco, M., Camerlenghi, A. (Eds.), Developments in Sedimentology. Elsevier, Oxford, pp. 511–535.

Krastel, S., Wefer, G., 2011. Sediment transport off Uruguay and Argentina: from the shelf to the deep sea. Meteorol. Ber., 58.

Krastel, S., Wefer, G., Hanebuth, T., Antobreh, A., Freudenthal, T., Preu, B., Schwenk, T., Strasser, M., Violante, R., Winkelmann, D., party, M.s.s., 2011. Sediment dynamics and geohazards off Uruguay and the de la Plata River region (northern Argentina and Uruguay). Geo-Mar. Lett. 31 (4), 271–283, http://dx.doi.org/10.1007/s00367-011-0232-4.

Krueger, S., Leuschner, D.C., Ehrmann, W., Schmiedl, G., Mackensen, A., 2012. North Atlantic Deep Water and Antarctic Bottom Water variability during the last 200 ka recorded in an abyssal sediment core off South Africa. Global Planet. Change 80–81, 180–189. http://dx.doi.org/10.1016/j.gloplacha.2011.10.001.

Laberg, J.S., Camerlenghi, A., 2008. The significance of contourites for submarine slope stability. Developments in sedimentology.. In: Rebesco, M., Camerlenghi, A. (Eds.), Contourites. Elsevier, pp. 537–556.

Lastras, G., Acosta, J., Munoz, A., Canals, M., 2011. Submarine canyon formation and evolution in the Argentine Continental Margin between 44°30′S and 48°S. Geomorphology 128, 116–136.

Le Pichon, X., Eittreim, S.L., Ludwig, W.J., 1971. Sediment transport and distribution in the Argentine Basin. 1. Antarctic Bottom current passage through the Falkland fracture zone. Phys. Chem. Earth 8 (0), 1–28, http://dx.doi.org/10.1016/0079-1946(71)90013-9.

Lonardi, A.G., Ewing, M., 1971. Sediment transport and distribution in the Argentine Basin. 4. Bathymetry of the continental margin, Argentine Basin and other related provinces. Canyons and sources of sediments. Phys. Chem. Earth 8, 79–121.

McCave, I.N., 1982. Erosion and deposition by currents on submarines slopes. Bull. Inst. Géol. Bassin d'Aquitaine 31, 47–55.

McCave, I.N., 2005. Deposition from suspension. In: Selley, R.C., Cocks, L.R.M., Malone, M.J. (Eds.), Encyclopedia of Geology. Elsevier, Oxford, pp. 8–17.

McCave, I.N., Hollister, C.D., Laine, E.P., Lonsdale, P.F., Richardson, M.J., 1982. Erosion and deposition on the eastern margin of the Bermuda Rise in the late Quaternary. Deep Sea Res. Part A 29 (5), 535–561, http://dx.doi.org/10.1016/0198-0149(82)90075-9.

McCave, I.N., Manighetti, B., Beveridge, N.A.S., 1995. Circulation in the glacial North Atlantic inferred from grain-size measurements. Nature 374 (6518), 149–152.

McCave, I.N., Tucholke, B.E., 1986. Deep current controlled sedimentation in the western Atlantic. In: Vogt, P.R., Tucholke, B.E. (Eds.), The Geology of North America. Geological Society of America, pp. 451–468.

Mulitza, S., Paul, A., Wefer, G., Scott, A.E., 2007. Late Pleistocene South Atlantic. Encyclopedia of Quaternary Science. Elsevier, Oxford, pp. 1816–1831.

Nelson, C.H., Baraza, J., Maldonado, A., 1993. Mediterranean undercurrent sandy contourites, Gulf of Cadiz, Spain. Sediment. Geol. 82 (1–4), 103–131, http://dx.doi.org/10.1016/0037-0738(93)90116-m.

Nelson, C.H., Baraza, J., Maldonado, A., Rodero, J., Escutia, C., Barber Jr, J.H., 1999. Influence of the Atlantic inflow and Mediterranean outflow currents on Late Quaternary sedimentary facies of the Gulf of Cadiz continental margin. Mar. Geol. 155 (1–2), 99–129, http://dx.doi.org/10.1016/s0025-3227(98)00143-1.

Ninnemann, U.S., Charles, C.D., 2002. Changes in the mode of Southern Ocean circulation over the last glacial cycle revealed by foraminiferal stable isotopic variability. Earth Planet. Sci. Lett. 201 (2), 383–396, http://dx.doi.org/10.1016/s0012-821x(02)00708-2.

Niño, Y., Lopez, F., Garcia, M., 2003. Threshold for particle entrainment into suspension. Sedimentology 50 (2), 247–263, http://dx.doi.org/10.1046/j.1365-3091.2003.00551.x.

Oppo, D., Fairbanks, R.G., 1987. Variability in the deep and intermediate water circulation of the Atlantic Ocean during the past 25,000 years: Northern Hemisphere modulation of the Southern Ocean. Earth Planet. Sci. Lett. 86, 1–15.

Parker, G., Paterlini, C.M., Violante, R., 1997. El fondo marino. In: Boschi, E. (Ed.), El Mar Argentino y sus Recursos Marinos, Mar del Plata, pp. 65–87.

Parker, G., Violante, R., Paterlini, C.M., 1996. Fisiografía de la Plataforma Continental. In: Ramos, V., Turic, M.A. (Eds.), Geología y Recursos Naturales de la Plataforma Continental Argentina. Buenos Aires, pp. 1–16.

Parker, G., Violante, R., Paterlini, C.M., Marcolini, S., Costa, I.P., Cavallotto, J.L., 2008. Las secuencias sismoestratigráficas del Plioceno-Cuaternario en la Plataforma Submarina adyacente al litoral del este bonaerense. Lat. Am. J. Sedimentol. Basin Anal. 15 (2), 105–124.

Piola, A.R., Matano, R.P., 2001. Brazil and Falklands (Malvinas) currents. Academic Press, London.

Piotrowski, A.M., Goldstein, S.L., Hemming, S.R., Fairbanks, R.G., Zylberberg, D.R., 2008. Oscillating glacial northern and southern deep water formation from combined neodymium and carbon isotopes. Earth Planet. Sci. Lett. 272 (1–2), 394–405, http://dx.doi.org/10.1016/j.epsl.2008.05.011.

Pomar, L., Morsilli, M., Hallock, P., Bádenas, B., 2012. Internal waves, an under-explored source of turbulence events in the sedimentary record. Earth Sci. Rev. 111, 56–81.

Potter, P.E., Szatmari, P., 2009. Global Miocene tectonics and the modern world. Earth Sci. Rev. 96 (4), 279–295, http://dx.doi.org/10.1016/j.earscirev.2009.07.003.

Preu, B., 2011. High-Resolution Seismo-Acoustic Studies of Alongslope and Downslope Sediment Transport Processes Shaping Depositional Patterns at Continental Margins. Ph.D. Thesis. University of Bremen. 128 pp.

Preu, B., Schwenk, T., Hernández-Molina, F.J., Violante, R., Paterlini, M., Krastel, S., Tomasini, J., Spieß, V., 2012. Sedimentary grwoth pattern on the northern Argentine slope: the impact of North Atlantic Deep Water on southern hemisphere slope architecture. Mar. Geol. 329–331, 113–125, http://dx.doi.org/10.1016/j.margeo.2012.09.009.

Preu, B., Spieß, V., Schwenk, T., Schneider, R., 2011. Evidence for current-controlled sedimentation along the southern Mozambique continental margin since Early Miocene times. Geo-Mar. Lett. 31 (5–6), 427–435, http://dx.doi.org/10.1007/s00367-011-0238-y.

Puig, P., Palanques, A., Guillén, J., El Khatab, M., 2004. Role of internal waves in the generation of nepheloid layers on the northwestern Alboran slope: implications for continental margin shaping. J. Geophys. Res. 109 (C9), C09011, http://dx.doi.org/10.1029/2004jc002394.

Ramos, V., 1999. Rasgos Estructurales del Territorio Argentino. Evolución Tectónica de la Argentina. In: Caminos, R. (Ed.), Geología Argentina. SEGEMAR. Buenos Aires, pp. 715–784.

Rasmussen, T.L., van Weering, T.C.E., Labeyrie, L., 1996. High resolution stratigraphy of the Faeroe–Shetland Channel and its relation to North Atlantic paleoceanography: the last 87 kyr. Mar. Geol. 131 (1–2), 75–88, http://dx.doi.org/10.1016/0025-3227(95)00145-x.

Rebesco, M., 2005. Contourites. In: Selley, R.C., Cocks, L.R.M., Plimer, I.R. (Eds.), Encyclopedia of Geology. Elsevier, Oxford, pp. 513–527.

Rebesco, M., Camerlenghi, A., 2008. Contourites. Developments in Sedimentology, 60. Elsevier 663 pp.

Reid, J.L., 1989. On the total geostrophic circulation of the Indian Ocean: flow patterns, tracers, and transports. Prog. Oceanogr. 23 (1), 149–244, http://dx.doi.org/10.1016/s0079-6611(02)00141-6.

Reid, J.L., Nowlin, W.D., Patzert, W.C., 1977. On the characteristics and circulation of the Southwestern Atlantic Ocean. J. Phys. Oceanogr. 7 (1), 62–91, http://dx.doi.org/10.1175/1520-0485(1977)007<0062:otcaco>2.0.co;2.

Ryan, W.B.F., Carbotte, S.M., Coplan, J.O., O'Hara, S., Melkonian, A., Arko, R., Weissel, R.A., Ferrini, V., Goodwillie, A., Nitsche, F., Bonczkowski, J., Zemsky, R., 2009. Global multi-resolution topography synthesis. Geochem. Geophys. Geosyst. 10 (3), Q03014, http://dx.doi.org/10.1029/2008gc002332.

Saraceno, M., Provost, C., Piola, A.R., Bava, J., Gagliardini, A., 2004. Brazil Malvinas Frontal System as seen from 9 years of advanced very high resolution radiometer data. J. Geophys. Res. 109 (C5), C05027, http://dx.doi.org/10.1029/2003jc002127.

Saunders, P.M., King, B.A., 1995. Oceanic Fluxes on the WOCE A11 Section. J. Phys. Oceanogr. 25 (9), 1942–1958, http://dx.doi.org/10.1175/1520-0485(1995)025<1942:ofotwa>2.0.co;2.

Schlitzer, R., 2011. Ocean Data View 4.0. 〈http://odv.awi.de〉.

Smith, W.H.F., Sandwell, D.T., 1997. Global Sea Floor Topography from Satellite Altimetry and Ship Depth Soundings. Science 277 (5334), 1956–1962, http://dx.doi.org/10.1126/science.277.5334.1956.

Spieß, V., Albrecht, N., Bickert, T., Breitzke, M., Brüning, M., Dreyzehner, A., Groß, U., Krüger, D., von Lom-Keil, H., Möller, H.-J., Nimrich, M., Ochsenhirt, W.-T., Rudolf, T., Seiter, C., Truscheit, T., Violante, R., Westerhold, T., 2002. ODP Südatlantik 2001 Part 2, Meteorol. Ber., 57.

Stow, D.A.V., Hernández-Molina, F.J., Llave, E., Sayago-Gil, M., Díaz del Ráo, V., Branson, A., 2009. Bedform-velocity matrix: the estimation of bottom current velocity from bedform observations. Geology 37 (4), 327–330, http://dx.doi.org/10.1130/g25259a.1.

Stow, D.A.V., Hunter, S., Wilkinson, D., Hernández-Molina, F.J., Rebesco, M., Camerlenghi, A., 2008. The nature of contourite deposition. In: Rebesco, Camerlenghi (Ed.), Developments in Sedimentology, 60. Elsevier, pp. 143–156.

Stow, D.A.V., Lovell, J.P.B., 1979. Contourites: Their recognition in modern and ancient sediments. Earth Sci. Rev. 14 (3), 251–291.

Stow, D.A.V., Mayall, M., 2000. Deep-water sedimentary systems: new models for the 21st century. Mar. Pet. Geol. 17 (2), 125–135.

Stow, D.A.V., Pudsey, C.J., Howe, J.A., Faugères, J.C., Viana, A.R., 2002. Deep-Water Contourite Systems: Modern Drifts and Ancient Series, Seismic and Sedimentary Characteristics. Geological Society, London.

Urien, C.M., Ewing, M., 1974. Recent sediments and environments of Southern Brazil, Uruguay, Buenos Aires and Rio Negro continental shelf. In: Burk, C.A. (Ed.), The Geology of Continental Margins. Springer, Berlin, pp. 1009.

Urien, C.M., Zambrano, J.J., 1996. Estructura del Margen Continental. In: Ramos, V., Turic, M.A. (Eds.), Geología y Recursos Naturales de la Plataforma Continental Argentina. Asociación Geológica Argentina-Instituto Argentino del Petróleo. Buenos Aires, pp. 29–65.

van Raaphorst, W., Malschaert, H., van Haren, H., Boer, W., Brummer, G., 2001. Cross-slope zonation of erosion and deposition in the Faeroe–Shetland Channel, North Atlantic Ocean. Deep Sea Res. Part A 48 (2), 567–591, http://dx.doi.org/10.1016/s0967-0637(00)00052-2.

Venz, K.A., Hodell, D.A., Stanton, C., Warnke, D.A., 1999. A 1.0 Myr record of glacial North Atlantic intermediate water variability from ODP Site 982 in the Northeast Atlantic. Paleoceanography 14 (1), 42–52, http://dx.doi.org/10.1029/1998pa900013.

Viana, A.R., 2008. Economic relevance of contourites. Developments in sedimentology.. In: Rebesco, Camerlenghi (Ed.), Developments in Sedimentology, 60. Elsevier, pp. 143–156, pp. 491, 493–510.

Viana, A.R., Faugères, J.-C., 1998. Upper Slope Sand Deposits: the Example of Campos Basin, a Latest Pleistocene-Holocene Record of the Interaction Between Alongslope and Downslope Currents, 129. Geological Society, London 287–316.

Viana, A.R., Hercos, C.M., Almeida Jr., W., Magalhães, J.L.C., Andrade, S.B., 2002. Evidence of bottom current influence on the neogene to quaternary sedimentation along the Northern Campos slope, SW Atlantic Margin. In: Stow, D.A.V., Pudsey, C.J., Howe, J.A., Faugeres, J-C, Viana, A R (Eds.), Deep-Water Contourite Systems: Modern Drifts and Ancient Series, Seismic and Sedimentary Characteristics, 22. Geological Society Memoir, pp. 249–259.

Violante, R.A., Parker, G., 2004. The post-last glacial maximum transgression in the de la Plata river and adjacent Inner continental shelf, Argentina. Quat. Int. 114 (1), 167–181.

Violante, R.A., Paterlini, C.M., Costa, I.P., Hernández-Molina, F.J., Segovia, L.M., Cavallotto, J.L., Marcolini, S., Bozzano, G., Laprida, C., García Chapori, N., Bickert, T., Spieß, V., 2010. Sismoestratigrafia y evolución geomorfológica del talud continental adyacente al litoral del este bonaerense, Argentina. Lat. Am. J. Sedimentol. Basin Anal 17, 33–62.

Weber, M.E., Bonani, G., Fütterer, K.D., 1994. Sedimentation processes within channel-ridge systems, Southeastern Weddell Sea, Antarctica. Paleoceanography 9 (6), 1027–1048, http://dx.doi.org/10.1029/94pa01443.

World Ocean Database, 2009. 〈http://www.nodc.noaa.gov/OC5/WOD/pr_wod.html〉.